Design by evolution

Peter Schuster

Institut für Theoretische Chemie, Universität Wien, Austria
and
The Santa Fe Institute, Santa Fe, New Mexico, USA

RNA 2006

Benasque, 17.– 27.07.2006

Web-Page for further information:

http://www.tbi.univie.ac.at/~pks

Evolution of RNA molecules based on Qβ phage

D.R.Mills, R,L,Peterson, S.Spiegelman, ***An extracellular Darwinian experiment with a self-duplicating nucleic acid molecule***. Proc.Natl.Acad.Sci.USA **58** (1967), 217-224

S.Spiegelman, ***An approach to the experimental analysis of precellular evolution***. Quart.Rev.Biophys. **4** (1971), 213-253

C.K.Biebricher, ***Darwinian selection of self-replicating RNA molecules***. Evolutionary Biology **16** (1983), 1-52

C.K.Biebricher, W.C. Gardiner, ***Molecular evolution of RNA* in vitro**. Biophysical Chemistry **66** (1997), 179-192

G.Strunk, T. Ederhof, ***Machines for automated evolution experiments* in vitro *based on the serial transfer concept***. Biophysical Chemistry **66** (1997), 193-202

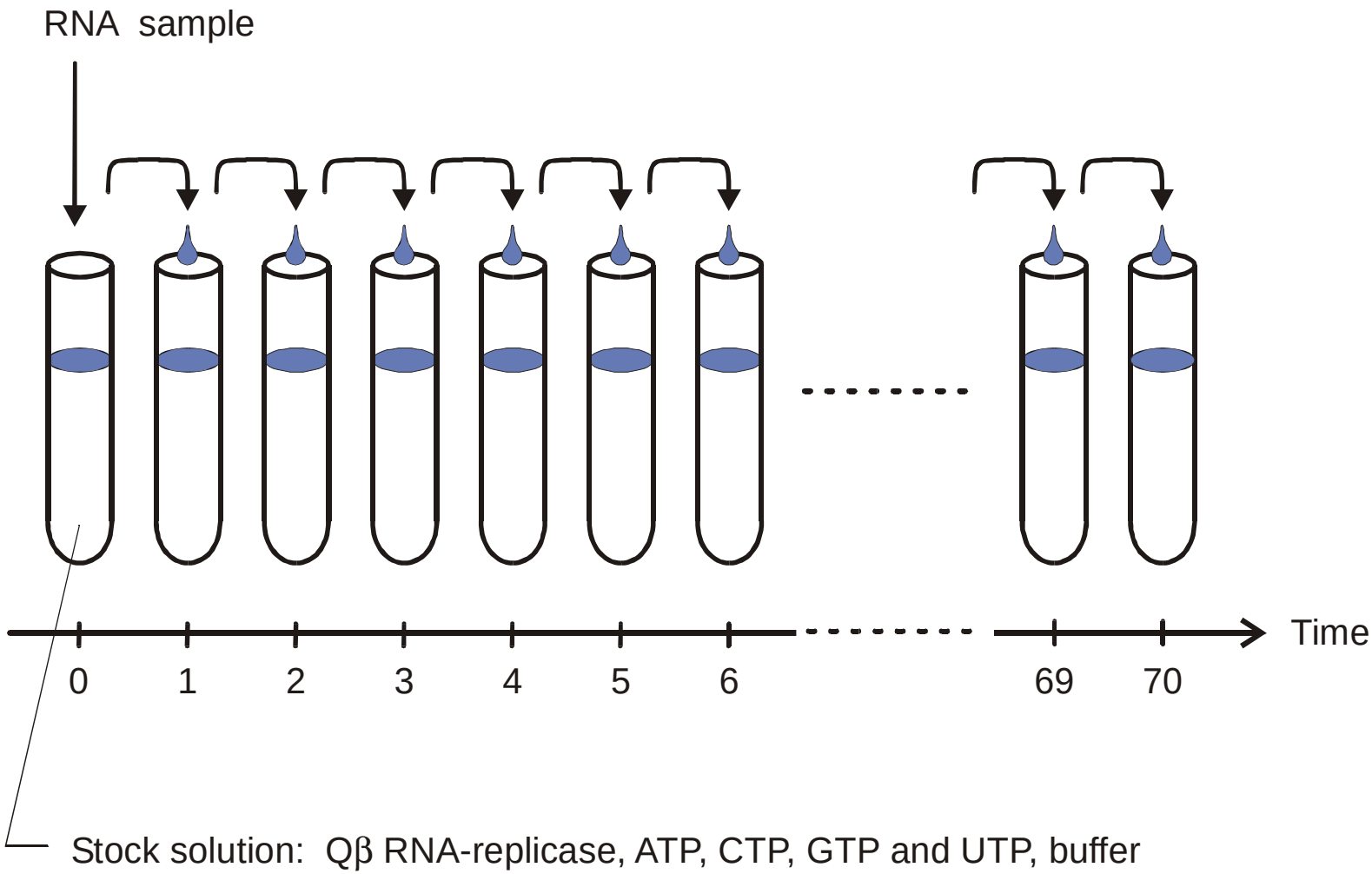

The serial transfer technique applied to RNA evolution ***in vitro***

Reproduction of the original figure of the serial transfer experiment with Qβ RNA

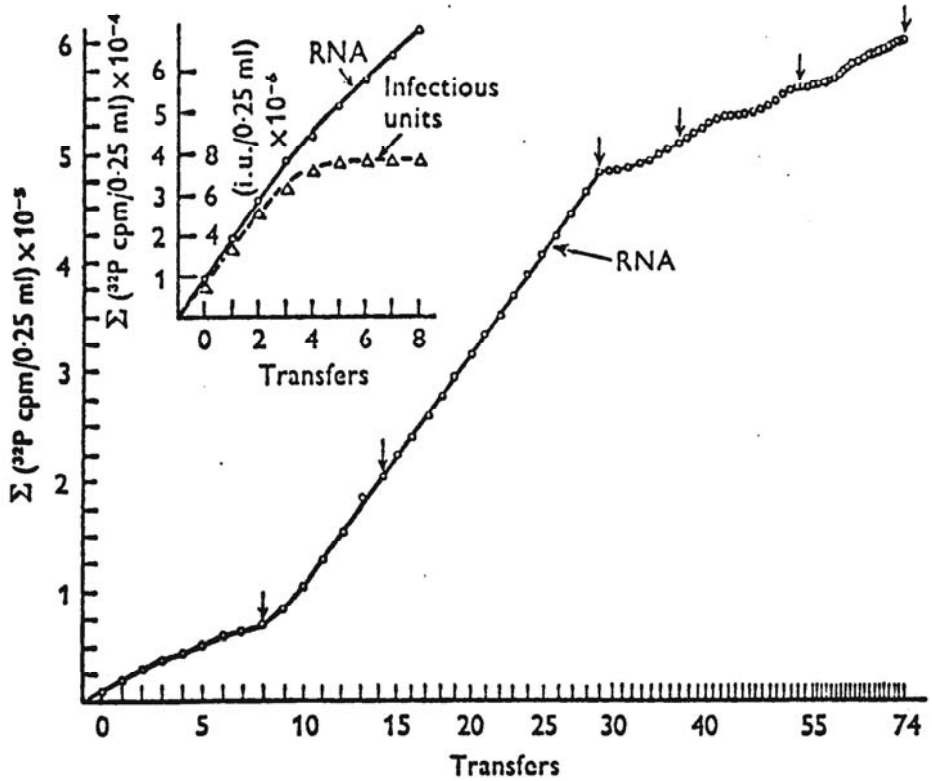

Fig. 9. Serial transfer experiment. Each 0·25 ml standard reaction mixture contained 40 μg of Qβ replicase and ³²P-UTP. The first reaction (0 transfer) was initiated by the addition of 0·2 μg ts-1 (temperature-sensitive RNA) and incubated at 35 °C for 20 min, whereupon 0·02 ml was drawn for counting and 0·02 ml was used to prime the second reaction (first transfer), and so on. After the first 13 reactions, the incubation periods were reduced to 15 min (transfers 14–29). Transfers 30–38 were incubated for 10 min. Transfers 39–52 were incubated for 7 min, and transfers 53–74 were incubated for 5 min. The arrows above certain transfers (0, 8, 14, 29, 37, 53, and 73) indicate where 0·001–0·1 ml of product was removed and used to prime reactions for sedimentation analysis on sucrose. The inset examines both infectious and total RNA. The results show that biologically competent RNA ceases to appear after the 4th transfer (Mills *et al.* 1967).

D.R.Mills, R,L,Peterson, S.Spiegelman, *An extracellular Darwinian experiment with a self-duplicating nucleic acid molecule*. Proc.Natl.Acad.Sci.USA **58** (1967), 217-224

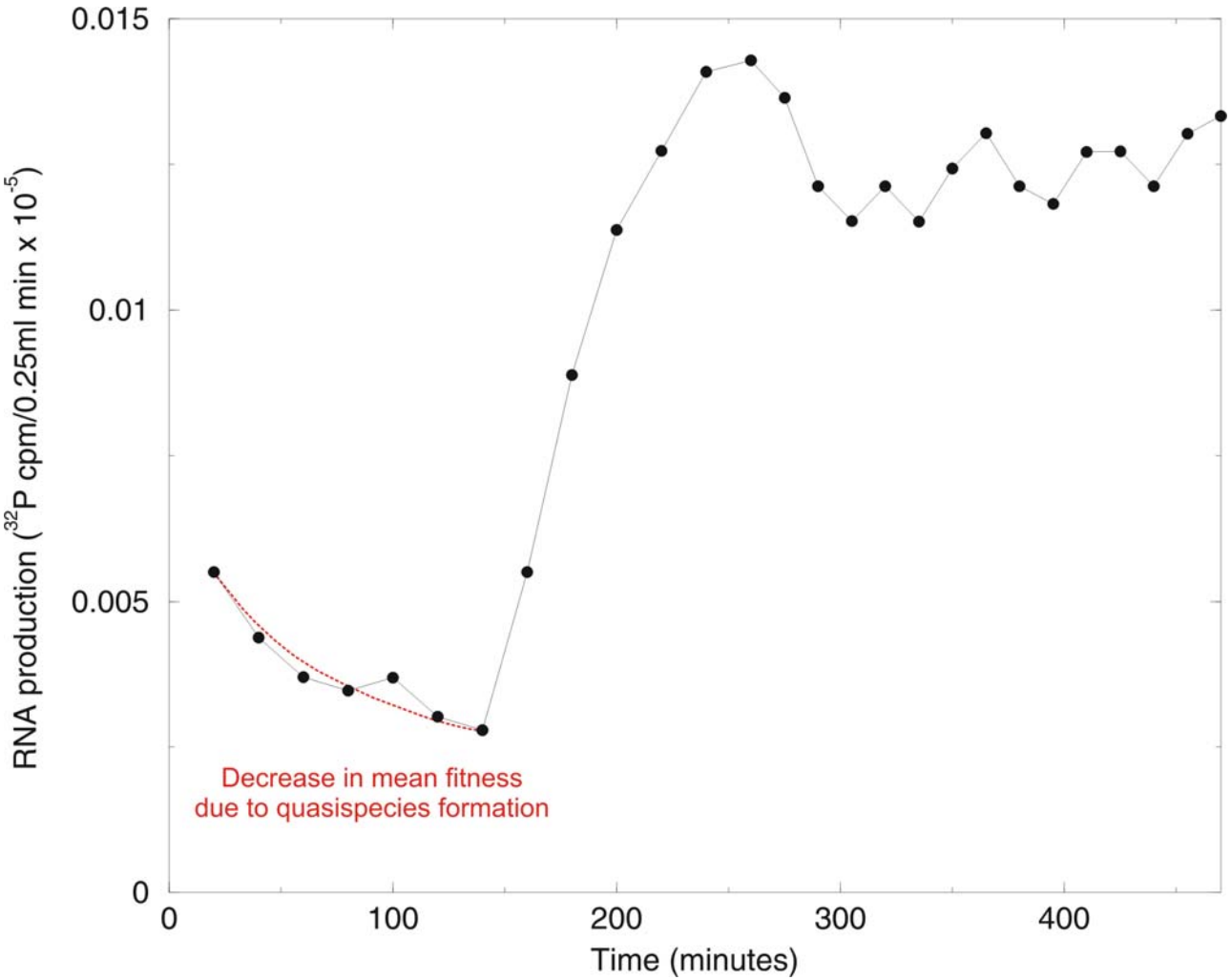

The increase in RNA production rate during a serial transfer experiment

Evolutionary design of RNA molecules

D.B.Bartel, J.W.Szostak, **In vitro *selection of RNA molecules that bind specific ligands***. Nature **346** (1990), 818-822

C.Tuerk, L.Gold, **SELEX - *Systematic evolution of ligands by exponential enrichment: RNA ligands to bacteriophage* T4 *DNA polymerase***. Science **249** (1990), 505-510

D.P.Bartel, J.W.Szostak, ***Isolation of new ribozymes from a large pool of random sequences***. Science **261** (1993), 1411-1418

R.D.Jenison, S.C.Gill, A.Pardi, B.Poliski, ***High-resolution molecular discrimination by RNA***. Science **263** (1994), 1425-1429

Y. Wang, R.R.Rando, ***Specific binding of aminoglycoside antibiotics to RNA***. Chemistry & Biology **2** (1995), 281-290

Jiang, A. K. Suri, R. Fiala, D. J. Patel, ***Saccharide-RNA recognition in an aminoglycoside antibiotic-RNA aptamer complex***. Chemistry & Biology **4** (1997), 35-50

An example of ‘artificial selection’ with RNA molecules or ‘breeding’ of biomolecules

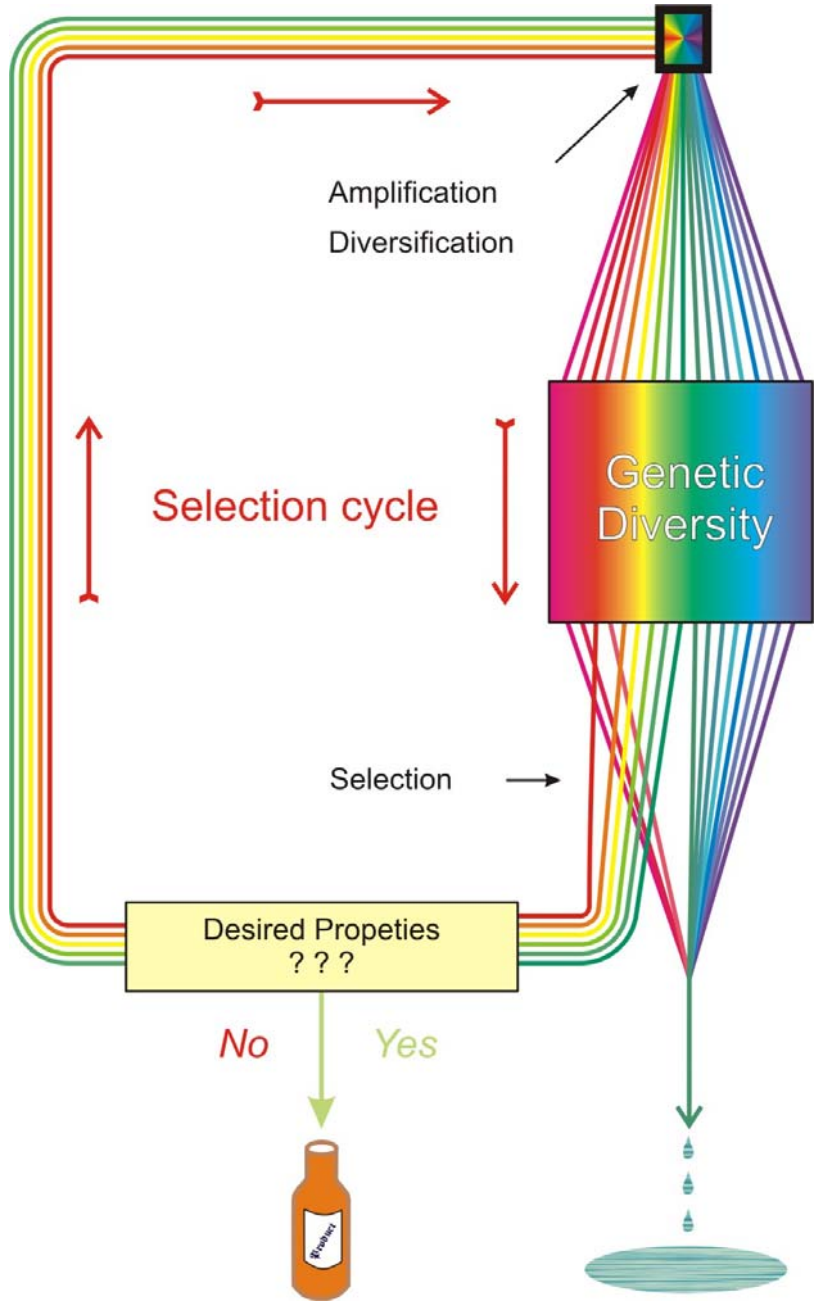

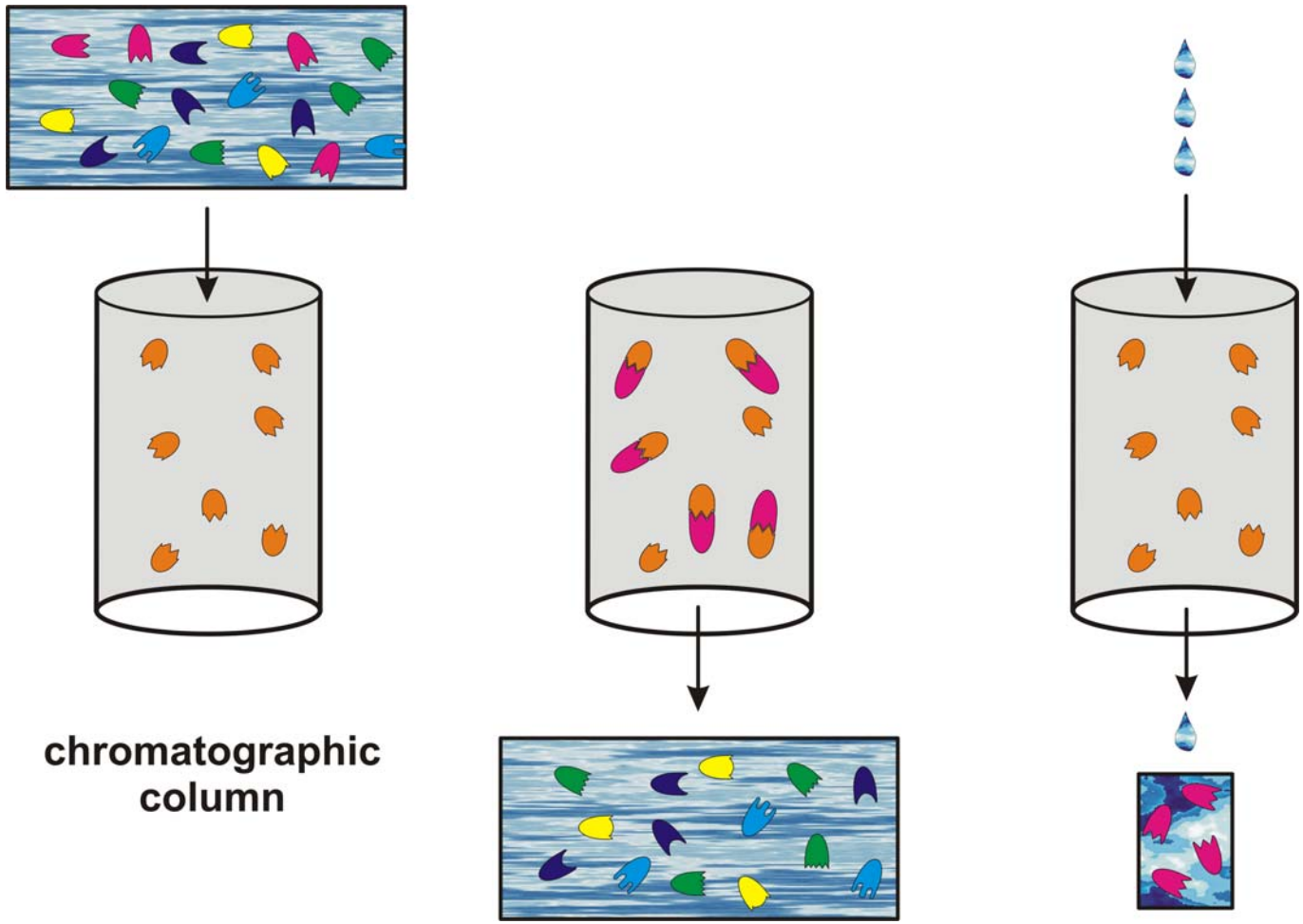

The SELEX technique for the evolutionary preparation of aptamers

additional methyl group

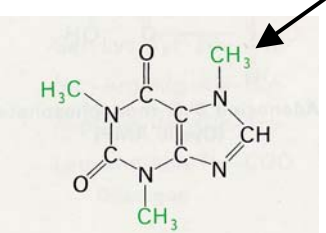

Caffeine
(1,3,7-Trimethylxanthine)

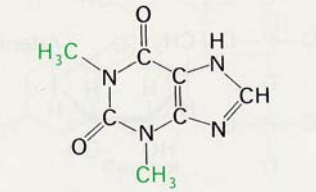

Theophylline
(1,3-Dimethylxanthine)

Dissociation constants and specificity of theophylline, caffeine, and related derivatives of uric acid for binding to a discriminating aptamer TCT8-4

Table 1. Competition binding analysis with TCT8-4 RNA. The chemical structures are shown for a series of derivatives used in competitive binding experiments with TCT8-4 RNA (Fig. 2) (*20*). The right column represents the affinity of the competitor relative to theophylline, $K_d(c)/K_d(t)$, where $K_d(c)$ is the individual competitor dissociation constant and $K_d(t)$ is the competitive dissociation constant of theophylline. Certain data (denoted by >) are minimum values that were limited by the solubility of the competitor. Each experiment was carried out in duplicate. The average error is shown.

Compound	Structure	$K_d(c)$ (μM)	$K_d(c)/K_d(t)$
Theophylline	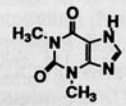	0.32 ± 0.13	1
CP-theophylline	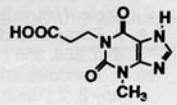	0.93 ± 0.20	2.9
Xanthine	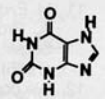	8.5 ± 0.40	27
1-Methylxanthine	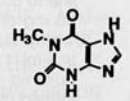	9.0 ± 0.30	28
3-Methylxanthine	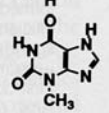	2.0 ± 0.7	6.3
7-Methylxanthine	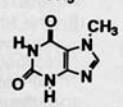	> 500	>1500
3,7-Dimethylxanthine	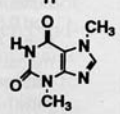	> 500	> 1500
1,3-Dimethyluric acid	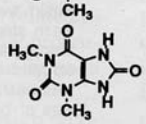	> 1000	>3100
Hypoxanthine	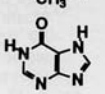	49 ± 10	153
Caffeine	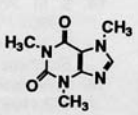	3500 ± 1500	10,900

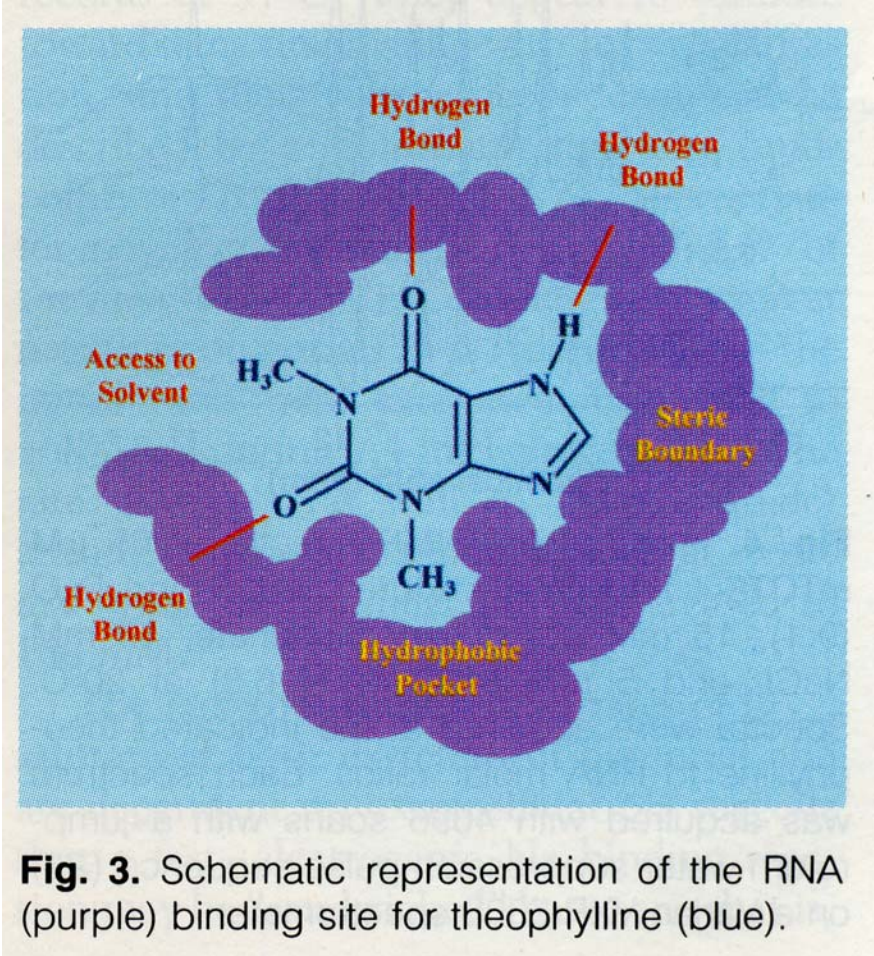

Fig. 3. Schematic representation of the RNA (purple) binding site for theophylline (blue).

Schematic drawing of the aptamer binding site for the theophylline molecule

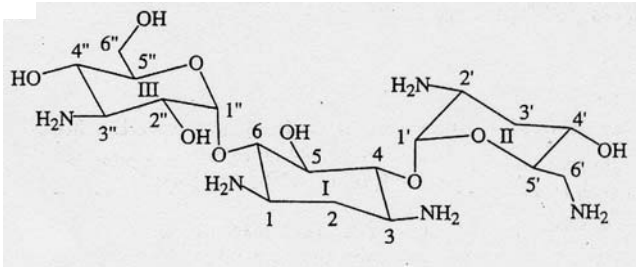

tobramycin

5’- G G C A C G A G G U U U A G C U A C A C U C G U G C C -3’

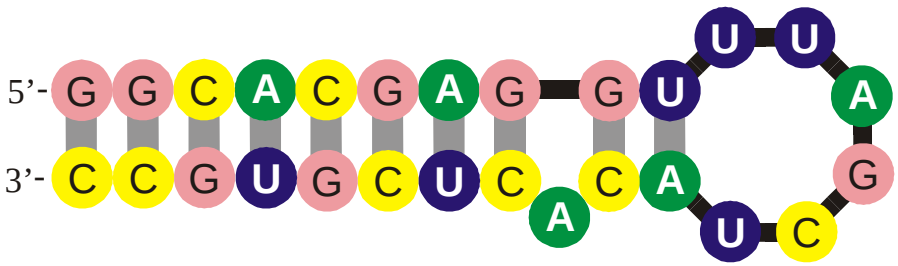

RNA aptamer

Formation of secondary structure of the tobramycin binding RNA aptamer with $K_D = 9$ nM

L. Jiang, A. K. Suri, R. Fiala, D. J. Patel, ***Saccharide-RNA recognition in an aminoglycoside antibiotic-RNA aptamer complex.*** Chemistry & Biology **4**:35-50 (1997)

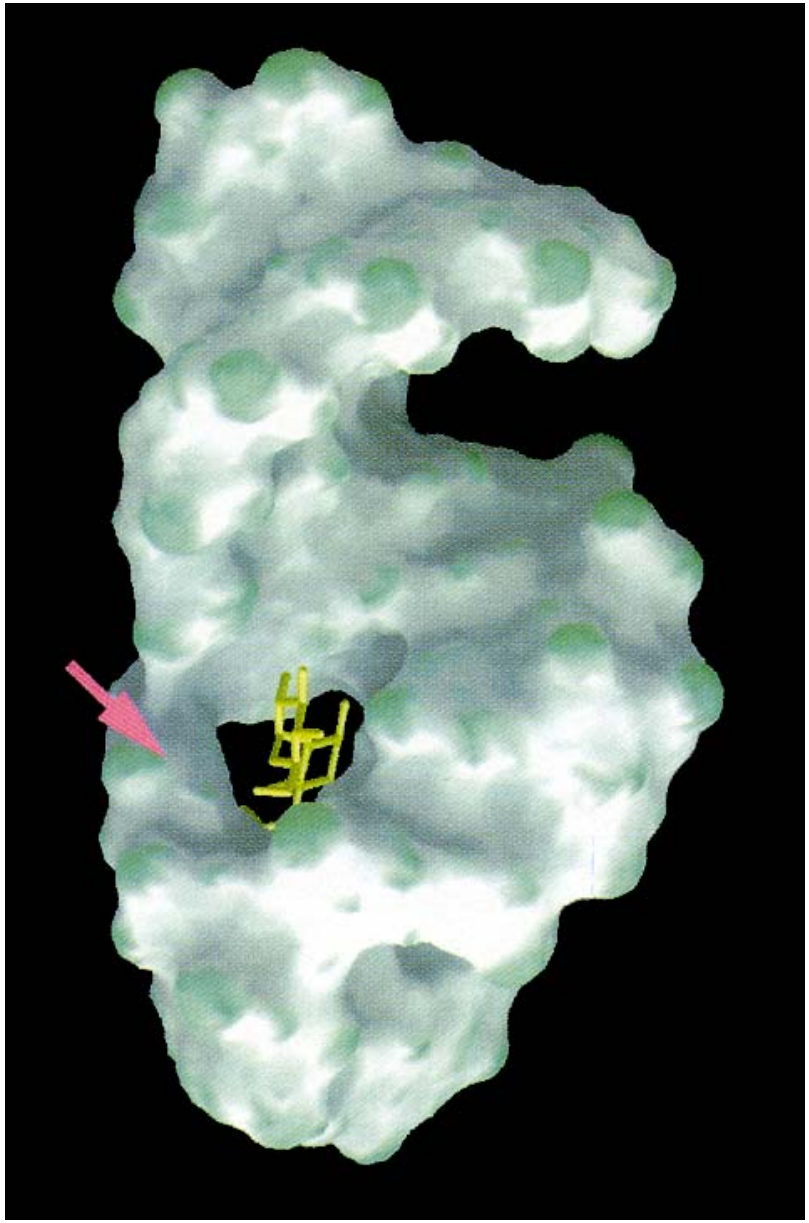

The three-dimensional structure of the tobramycin aptamer complex

L. Jiang, A. K. Suri, R. Fiala, D. J. Patel, Chemistry & Biology **4**:35-50 (1997)

No new principle will declare itself from below a heap of facts.

Sir Peter Medawar, 1985

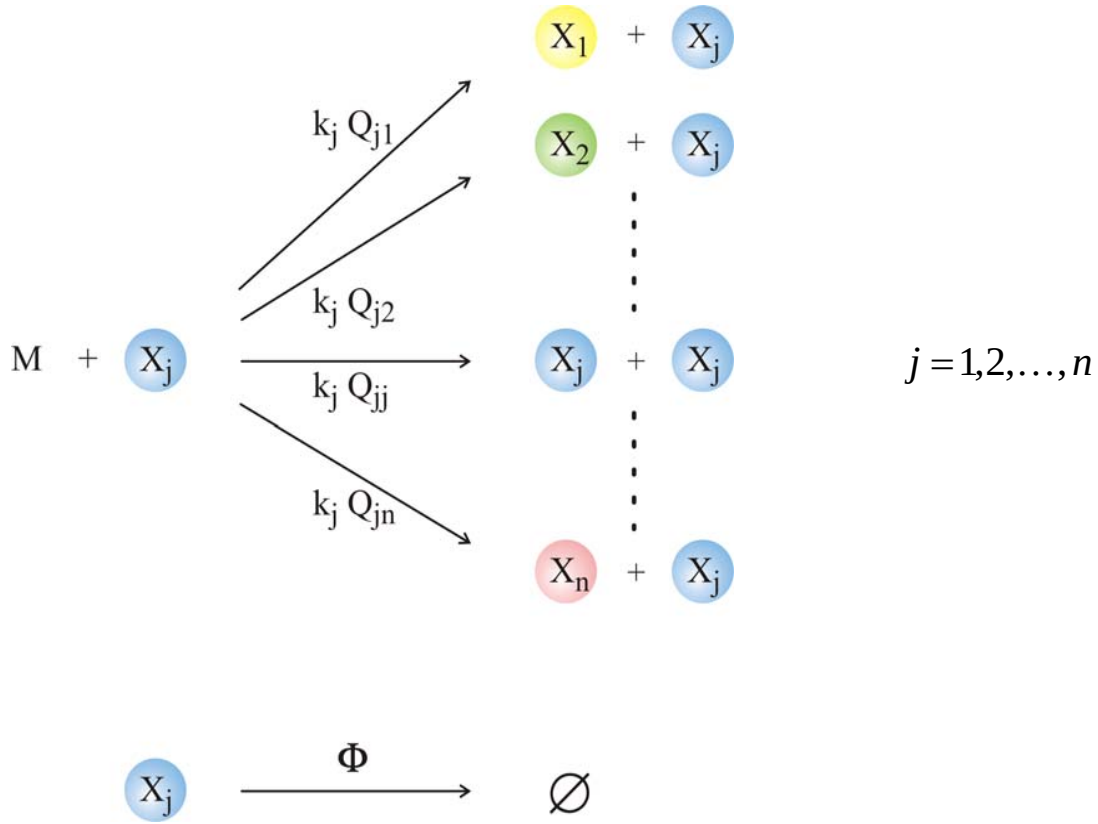

$$\frac{dx_j}{dt} = \sum_{i=1}^{n} f_j Q_{ij} x_i - x_j \Phi \quad \text{with} \quad \Phi = \sum_{i=1}^{n} f_i x_i \quad \text{and} \quad \sum_{i=1}^{n} x_i = 1$$

Replication and mutation in the flowreactor

$Q_{ij} = (1-p)^{n-d_H(X_i,X_j)}\, p^{d_H(X_i,X_j)}$; p … error rate per digit and replication

$d_H(X_i,X_j)$ … Hamming distance between X_i and X_j; $\sum_{j=1}^{n} Q_{ij} = 1$

Evolution of RNA molecules as a Markow process and its analysis by means of the relay series

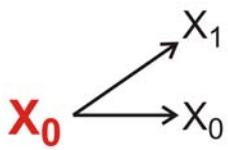

Evolution of RNA molecules as a Markow process and its analysis by means of the relay series

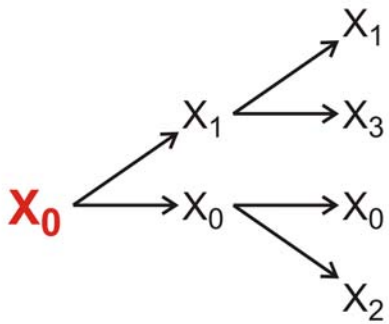

Evolution of RNA molecules as a Markow process and its analysis by means of the relay series

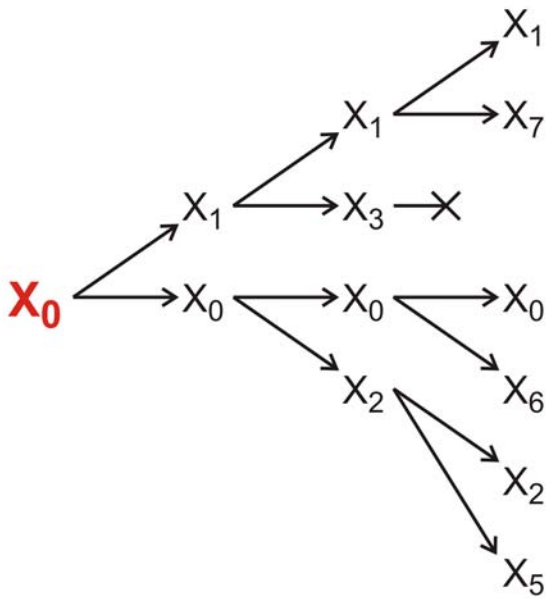

Evolution of RNA molecules as a Markow process and its analysis by means of the relay series

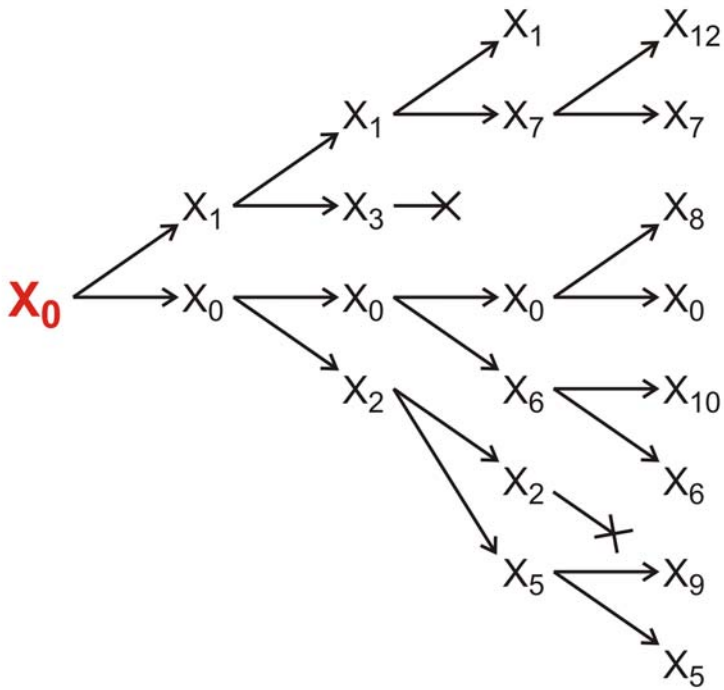

Evolution of RNA molecules as a Markow process and its analysis by means of the relay series

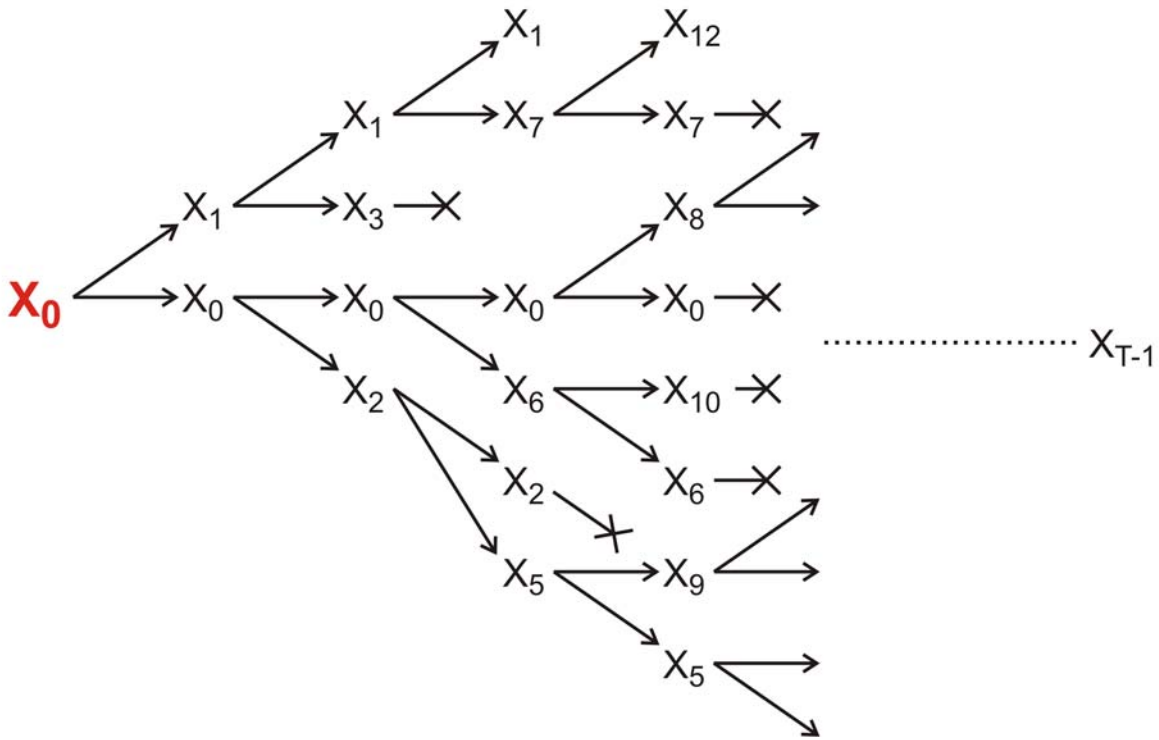

Evolution of RNA molecules as a Markow process and its analysis by means of the relay series

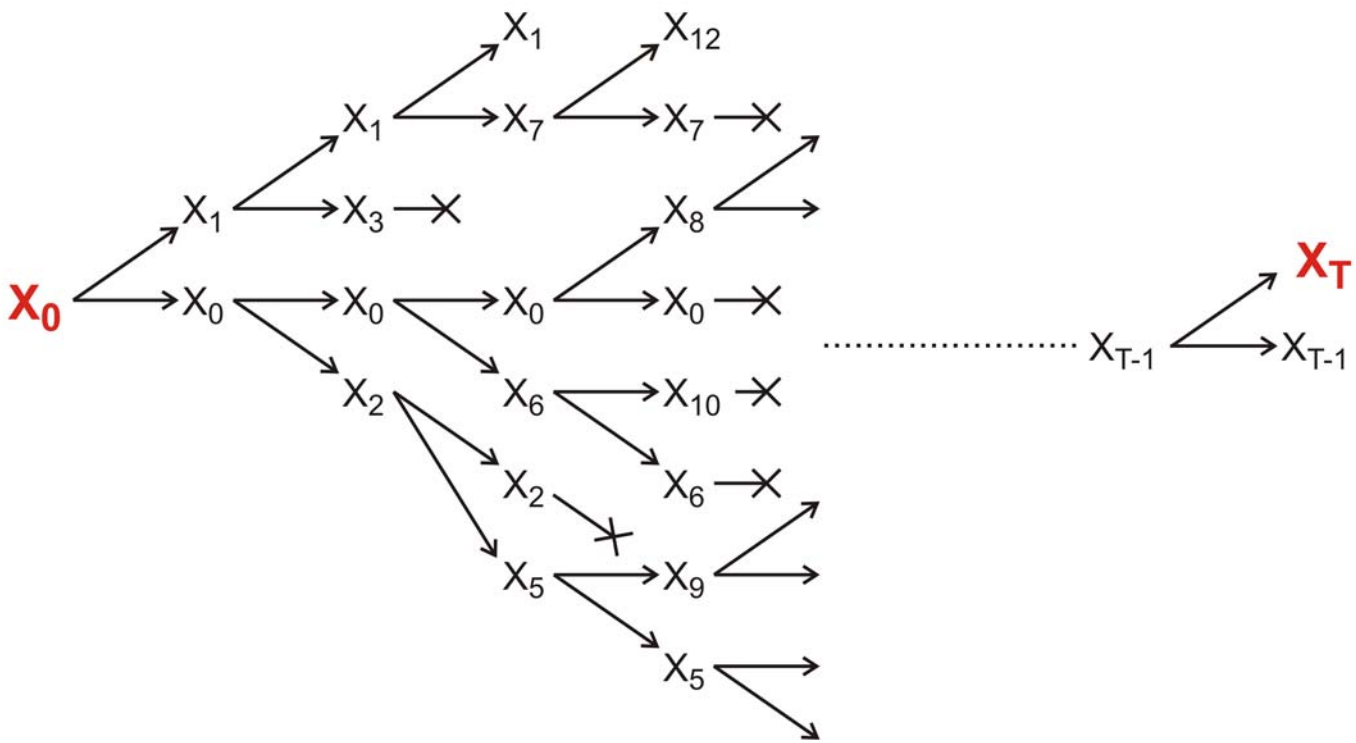

Evolution of RNA molecules as a Markow process and its analysis by means of the relay series

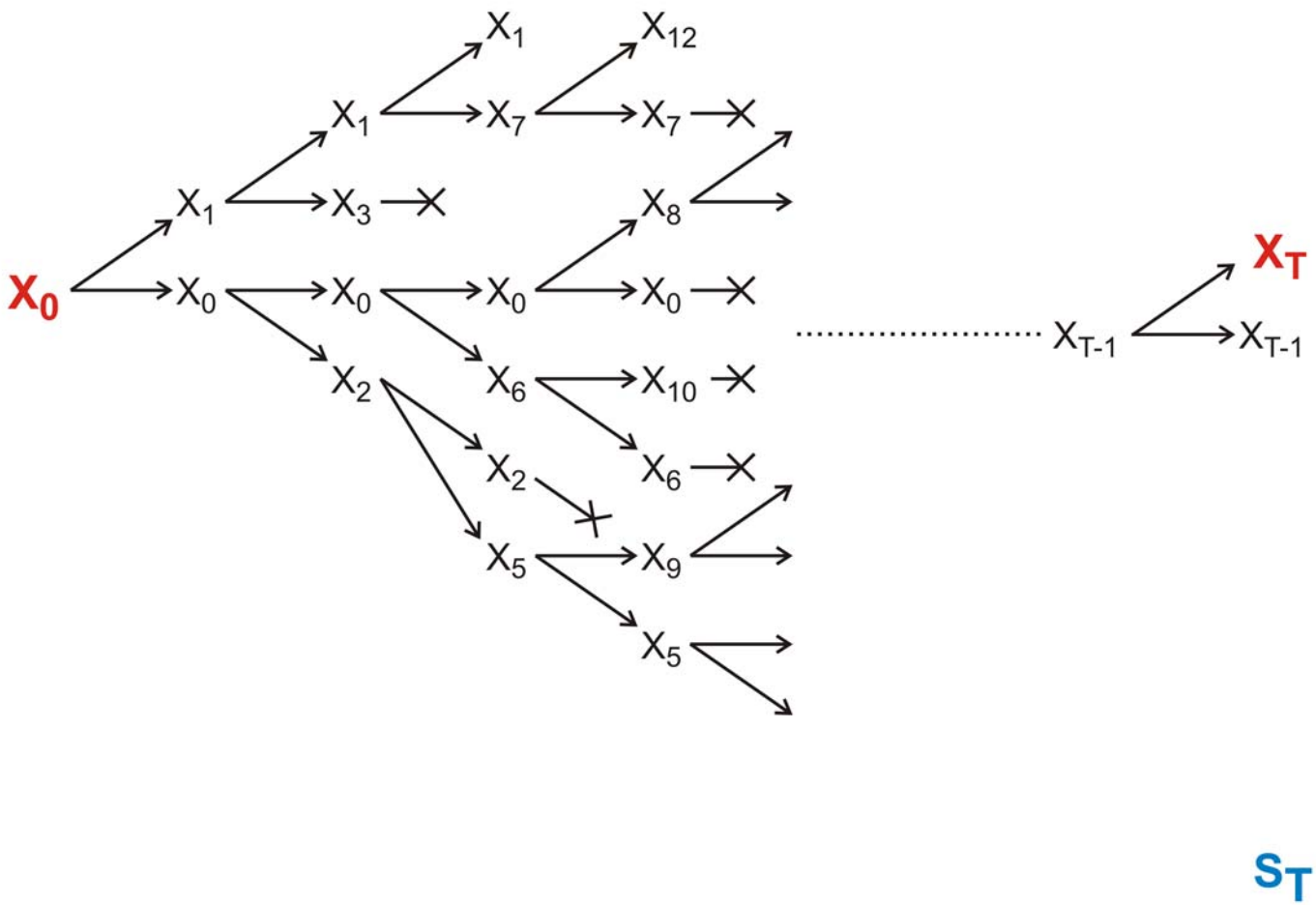

Evolution of RNA molecules as a Markow process and its analysis by means of the relay series

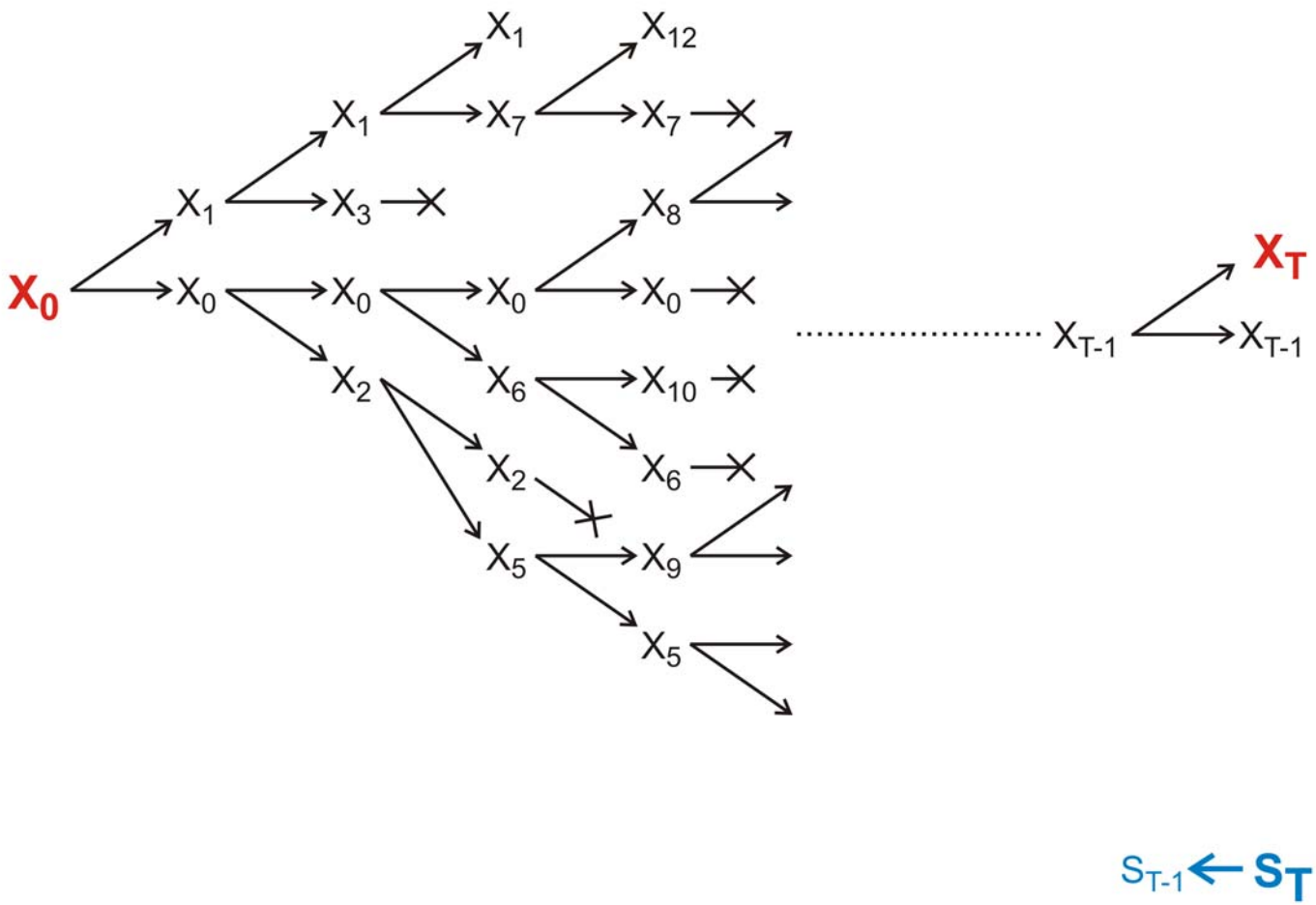

Evolution of RNA molecules as a Markow process and its analysis by means of the relay series

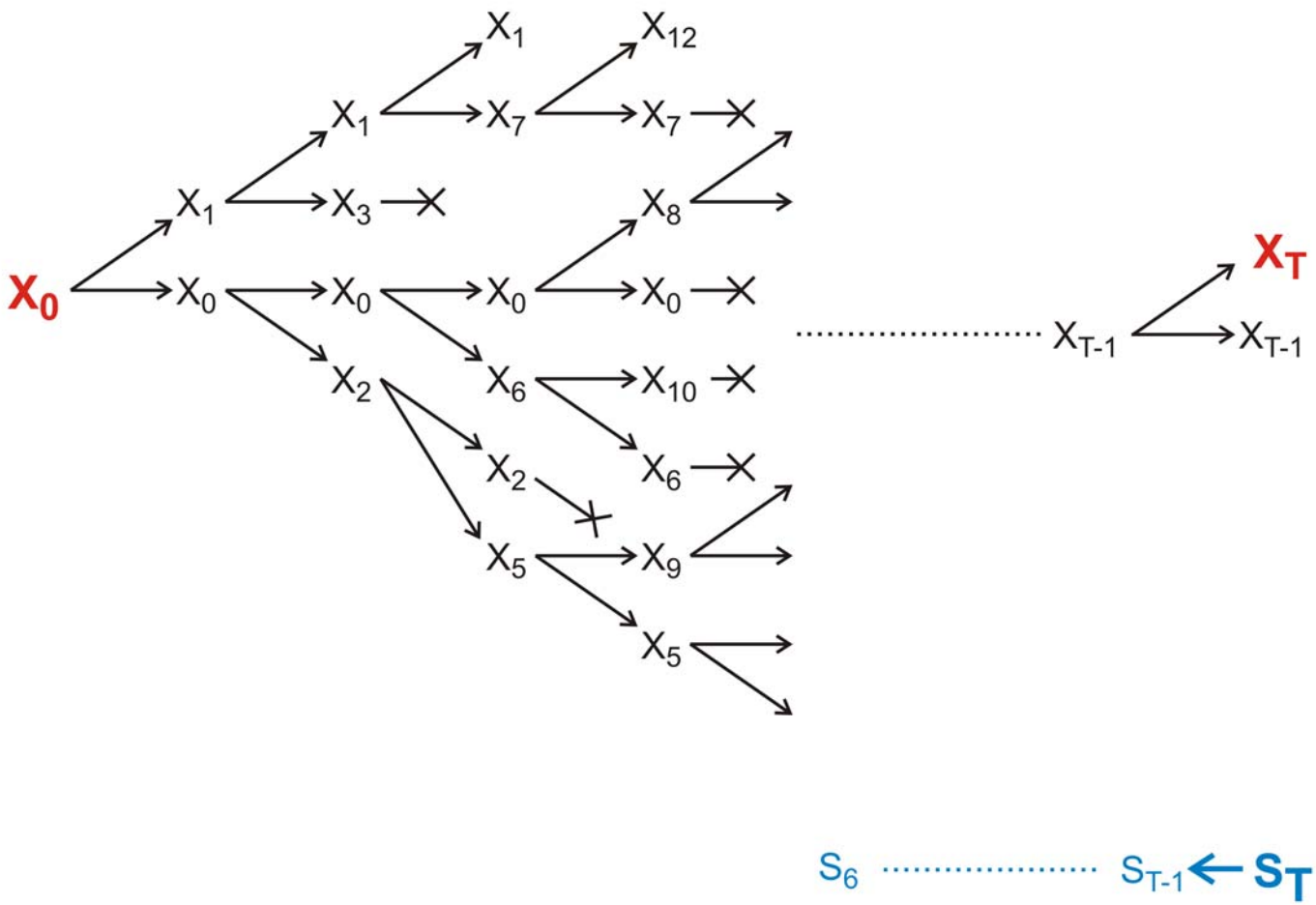

Evolution of RNA molecules as a Markow process and its analysis by means of the relay series

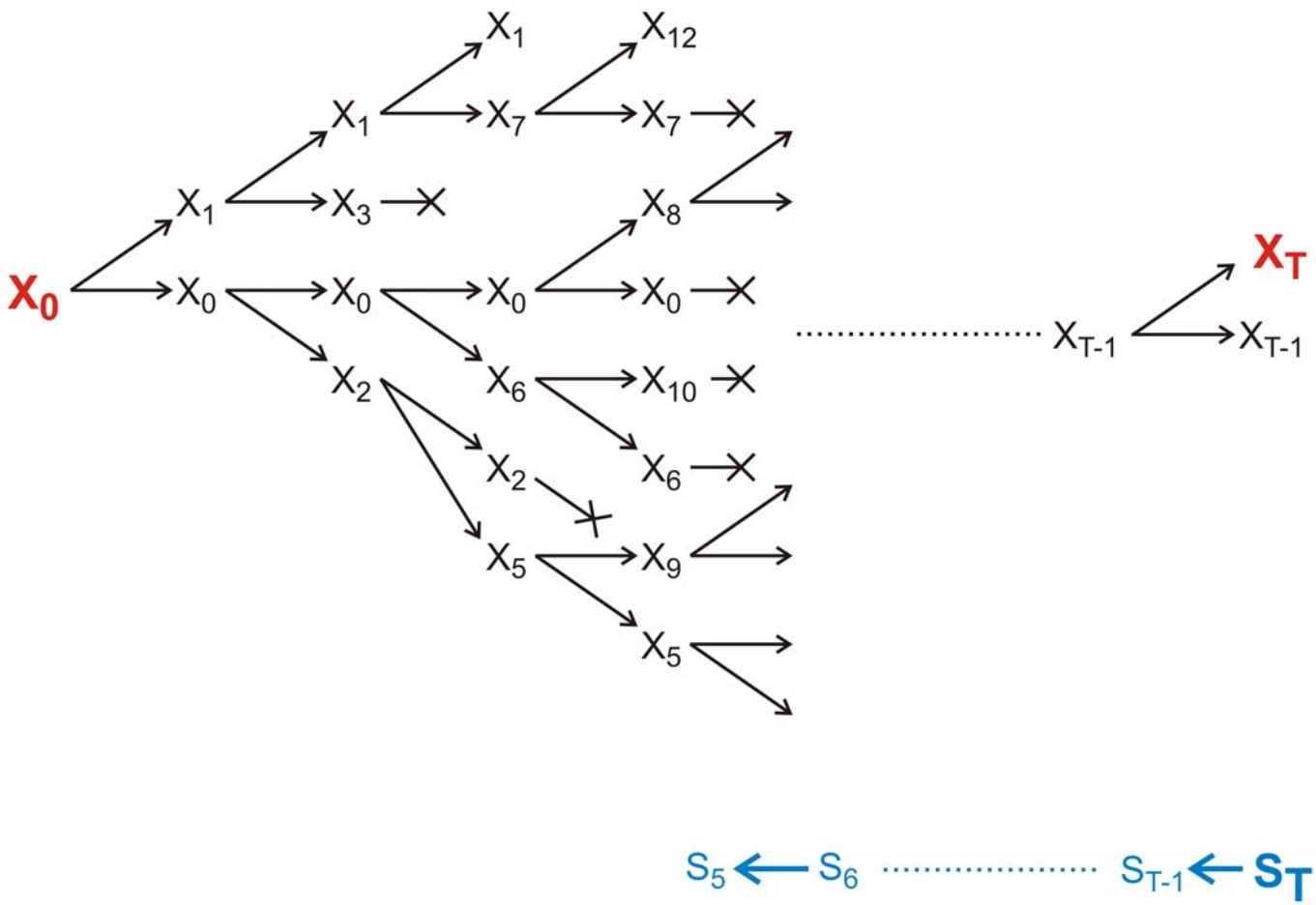

Evolution of RNA molecules as a Markow process and its analysis by means of the relay series

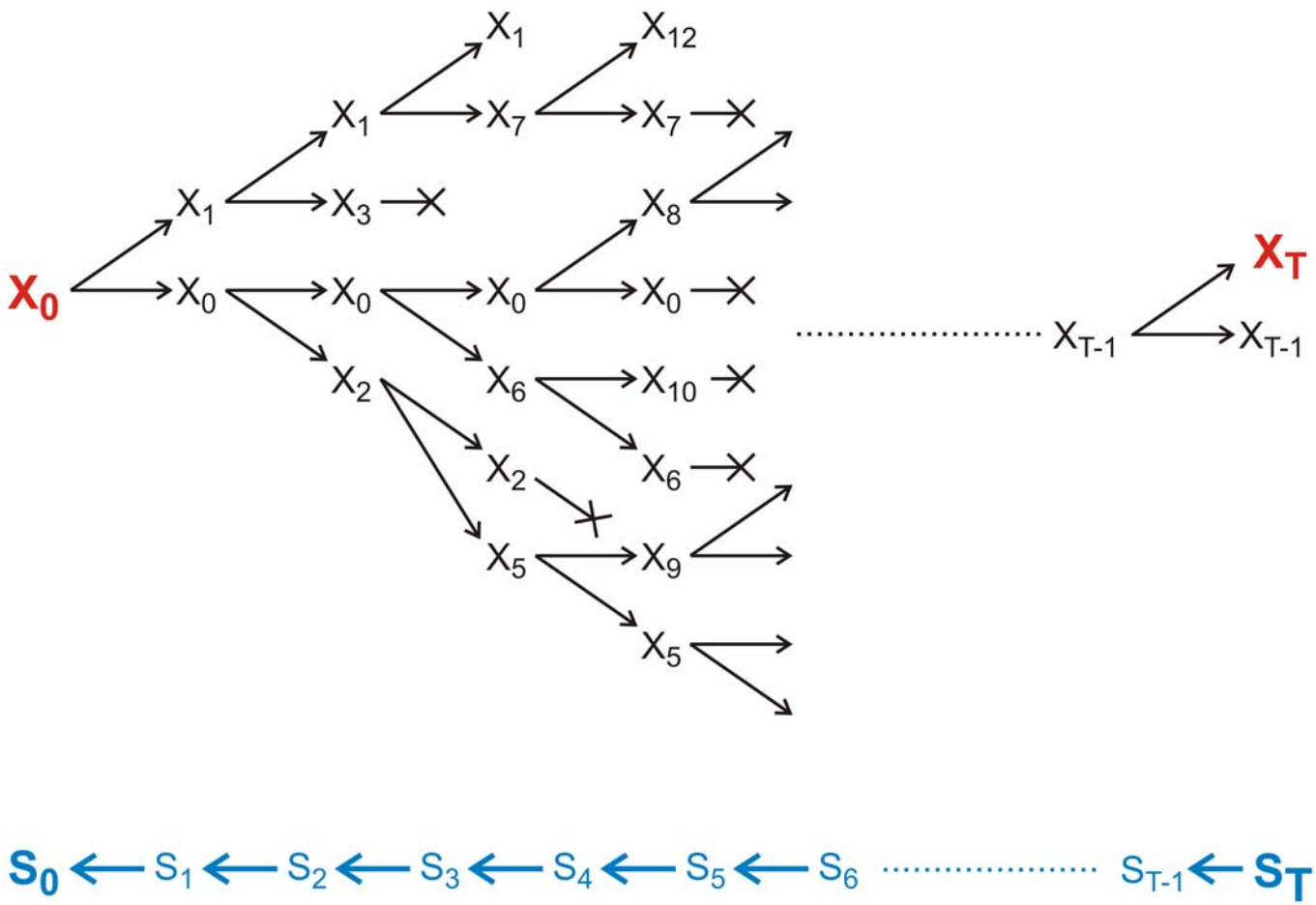

Evolution of RNA molecules as a Markow process and its analysis by means of the relay series

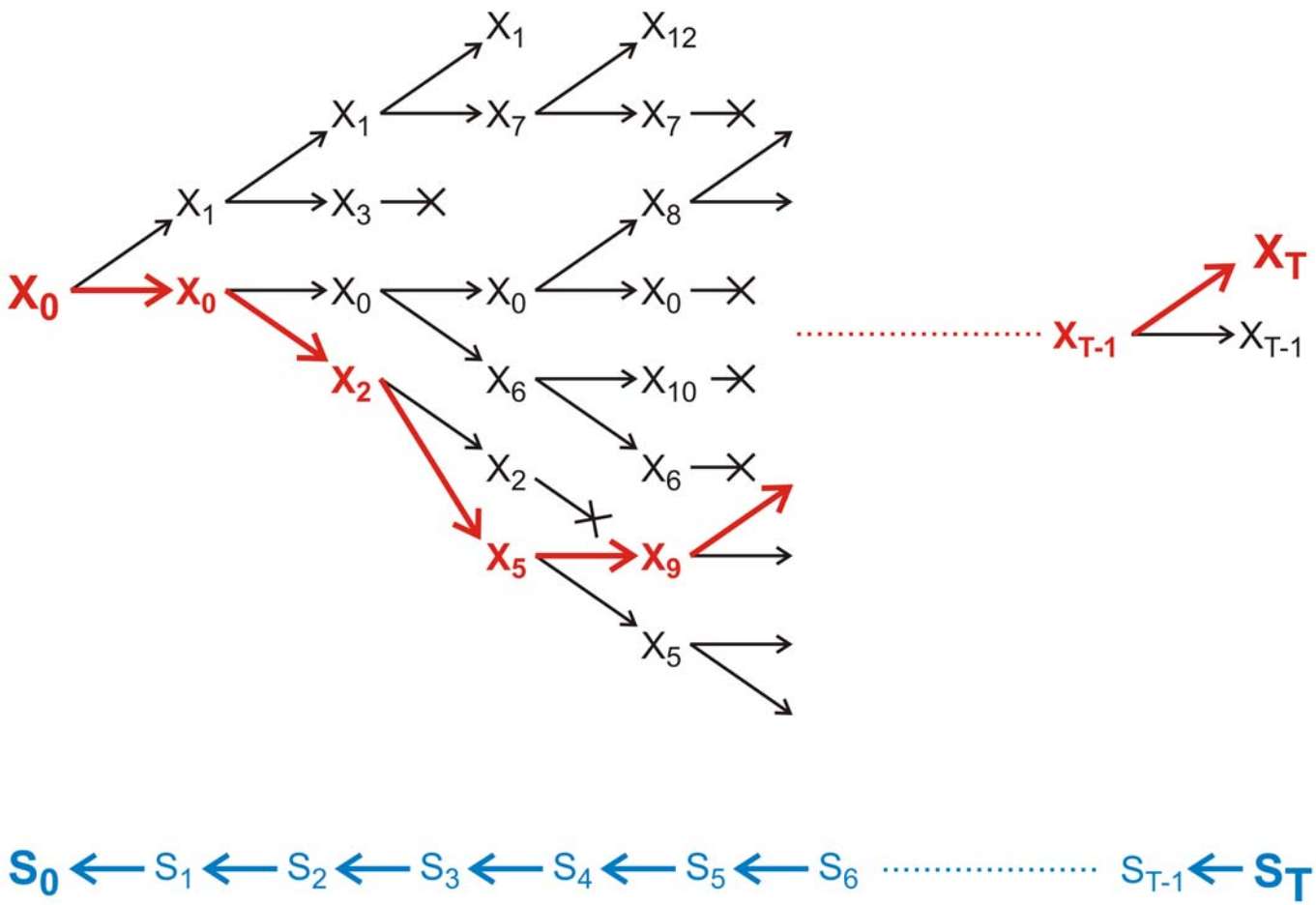

Evolution of RNA molecules as a Markow process and its analysis by means of the relay series

Evolution *in silico*

W. Fontana, P. Schuster,
Science **280** (1998), 1451-1455

random individuals. The primer pair used for genomic DNA amplification is 5′-TCTCCCTGGATTCT-CATTTA-3′ (forward) and 5′-TCTTTGTCTTCTGT-TCCACC-3′ (reverse). Reactions were performed in 25 μl using 1 unit of Taq DNA polymerase with each primer at 0.4 μM; 200 μM each dATP, dTTP, dGTP, and dCTP; and PCR buffer [10 mM tris-HCl (pH 8.3), 50 mM KCl_2,1.5 mM $MgCl_2$] in a cycle condition of 94°C for 1 min and then 35 cycles of 94°C for 30 s, 55°C for 30 s, and 72°C for 30 s followed by 72°C for 6 min. PCR products were purified (Qiagen), digested with Xmn I, and separated in a 2% agarose gel.

32. A nonsense mutation may affect mRNA stability and result in degradation of the transcript [L. Maquat, *Am. J. Hum. Genet.* **59**, 279 (1996)].
33. Data not shown; a dot blot with poly (A)$^+$ RNA from 50 human tissues (The Human RNA Master Blot, 7770-1, Clontech Laboratories) was hybridized with a probe from exons 29 to 47 of *MYO15* using the same condition as Northern blot analysis (*13*).
34. Smith–Magenis syndrome (SMS) is due to deletions of 17p11.2 of various sizes, the smallest of which includes *MYO15* and perhaps 20 other genes [(*6*); K-S Chen, L. Potocki, J. R. Lupski, *MRDD Res. Rev.* **2**, 122 (1996)]. *MYO15* expression is easily detected in the pituitary gland (data not shown). Haploinsufficiency for *MYO15* may explain a portion of the SMS phenotype such as short stature. Moreover, a few SMS patients have sensorineural hearing loss, possibly because of a point mutation in *MYO15* in trans to the SMS 17p11.2 deletion.
35. R. A. Fridell, data not shown.
36. K. B. Avraham *et al.*, *Nature Genet.* **11**, 369 (1995); X-Z. Liu *et al.*, *ibid.* **17**, 268 (1997); F. Gibson *et al.*, *Nature* **374**, 62 (1995); D. Weil *et al.*, *ibid.*, p. 60.
37. RNA was extracted from cochlea (membranous labyrinths) obtained from human fetuses at 18 to 22 weeks of development in accordance with guidelines established by the Human Research Committee at the Brigham and Women's Hospital. Only samples without evidence of degradation were pooled for poly (A)$^+$ selection over oligo(dT) columns. First-strand cDNA was prepared using an Advantage RT-for-PCR kit (Clontech Laboratories). A portion of the first-strand cDNA (4%) was amplified by PCR with Advantage cDNA polymerase mix (Clontech Laboratories) using human *MYO15*-specific oligonucleotide primers (forward, 5′-GCATGACCTGCCGGCTAAT-GGG-3′; reverse, 5′-CTCACGGCTTCTGCATGGT-GCTCGGCTGGC-3′). Cycling conditions were 40 s at 94°C; 40 s at 66°C (3 cycles), 60°C (5 cycles), and 55°C (29 cycles); and 45 s at 68°C. PCR products were visualized by ethidium bromide staining after fractionation in a 1% agarose gel. A 688-bp PCR product is expected from amplification of the human *MYO15* cDNA. Amplification of human genomic DNA with this primer pair would result in a 2903-bp fragment.

38. We are grateful to the people of Bengkala, Bali, and the two families from India. We thank J. R. Lupski and K.-S. Chen for providing the human chromosome 17 cosmid library. For technical and computational assistance, we thank N. Dietrich, M. Fergusson, A. Gupta, E. Sorbello, R. Torkzadeh, C. Varner, M. Walker, G. Bouffard, and S. Beckstrom-Sternberg (National Institutes of Health Intramural Sequencing Center). We thank J. T. Hinnant, I. N. Arhya, and S. Winata for assistance in Bali, and T. Barber, S. Sullivan, E. Green, D. Drayna, and J. Battey for helpful comments on this manuscript. Supported by the National Institute on Deafness and Other Communication Disorders (NIDCD) (Z01 DC 00035-01 and Z01 DC 00038-01 to T.B.F. and E.R.W. and R01 DC 03402 to C.C.M.), the National Institute of Child Health and Human Development (R01 HD30428 to S.A.C.) and a National Science Foundation Graduate Research Fellowship to F.J.P. This paper is dedicated to J. B. Snow Jr. on his retirement as the Director of the NIDCD.

9 March 1998; accepted 17 April 1998

Continuity in Evolution: On the Nature of Transitions

Walter Fontana and Peter Schuster

To distinguish continuous from discontinuous evolutionary change, a relation of nearness between phenotypes is needed. Such a relation is based on the probability of one phenotype being accessible from another through changes in the genotype. This nearness relation is exemplified by calculating the shape neighborhood of a transfer RNA secondary structure and provides a characterization of discontinuous shape transformations in RNA. The simulation of replicating and mutating RNA populations under selection shows that sudden adaptive progress coincides mostly, but not always, with discontinuous shape transformations. The nature of these transformations illuminates the key role of neutral genetic drift in their realization.

A much-debated issue in evolutionary biology concerns the extent to which the history of life has proceeded gradually or has been punctuated by discontinuous transitions at the level of phenotypes (*1*). Our goal is to make the notion of a discontinuous transition more precise and to understand how it arises in a model of evolutionary adaptation.

We focus on the narrow domain of RNA secondary structure, which is currently the simplest computationally tractable, yet realistic phenotype (*2*). This choice enables the definition and exploration of concepts that may prove useful in a wider context. RNA secondary structures represent a coarse level of analysis compared with the three-dimensional structure at atomic resolution. Yet, secondary structures are empirically well defined and obtain their biophysical and biochemical importance from being a scaffold for the tertiary structure. For the sake of brevity, we shall refer to secondary structures as "shapes." RNA combines in a single molecule both genotype (replicatable sequence) and phenotype (selectable shape), making it ideally suited for in vitro evolution experiments (*3*, *4*).

To generate evolutionary histories, we used a stochastic continuous time model of an RNA population replicating and mutating in a capacity-constrained flow reactor under selection (*5*, *6*). In the laboratory, a goal might be to find an RNA aptamer binding specifically to a molecule (*4*). Although in the experiment the evolutionary end product was unknown, we thought of its shape as being specified implicitly by the imposed selection criterion. Because our intent is to study evolutionary histories rather than end products, we defined a target shape in advance and assumed the replication rate of a sequence to be a function of the similarity between its shape and the target. An actual situation may involve more than one best shape, but this does not affect our conclusions.

An instance representing in its qualitative features all the simulations we performed is shown in Fig. 1A. Starting with identical sequences folding into a random shape, the simulation was stopped when the population became dominated by the target, here a canonical tRNA shape. The black curve traces the average distance to the target (inversely related to fitness) in the population against time. Aside from a short initial phase, the entire history is dominated by steps, that is, flat periods of no apparent adaptive progress, interrupted by sudden approaches toward the target structure (*7*). However, the dominant shapes in the population not only change at these marked events but undergo several fitness-neutral transformations during the periods of no apparent progress. Although discontinuities in the fitness trace are evident, it is entirely unclear when and on the basis of what the series of successive phenotypes itself can be called continuous or discontinuous.

A set of entities is organized into a (topological) space by assigning to each entity a system of neighborhoods. In the present case, there are two kinds of entities: sequences and shapes, which are related by a thermodynamic folding procedure. The set of possible sequences (of fixed length) is naturally organized into a space because point mutations induce a canonical neighborhood. The neighborhood of a sequence consists of all its one-error mutants. The problem is how to organize the set of possible shapes into a space. The issue arises because, in contrast to sequences, there are

Institut für Theoretische Chemie, Universität Wien, Währingerstrasse 17, A-1090 Wien, Austria, Santa Fe Institute, 1399 Hyde Park Road, Santa Fe, NM 87501, USA, and International Institute for Applied Systems Analysis (IIASA), A-2361 Laxenburg, Austria.

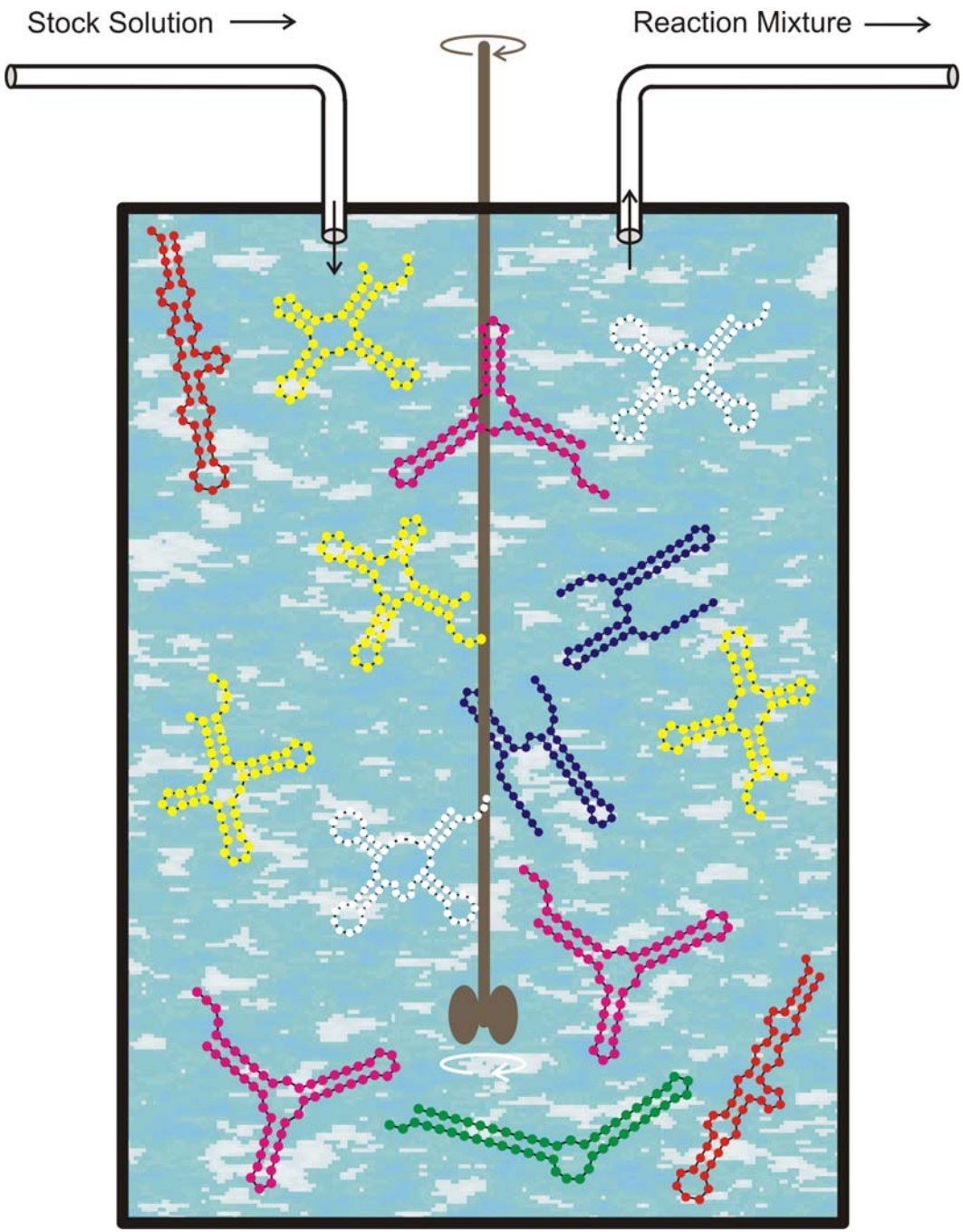

Replication rate constant:

$$f_k = \gamma / [\alpha + \Delta d_S^{(k)}]$$

$$\Delta d_S^{(k)} = d_H(S_k, S_\tau)$$

Selection constraint:

Population size, N = # RNA molecules, is controlled by the flow

$$N(t) \approx \overline{N} \pm \sqrt{\overline{N}}$$

Mutation rate:

p = 0.001 / site × replication

The flowreactor as a device for **studies** of evolution ***in vitro*** and ***in silico***

Randomly chosen
initial structure

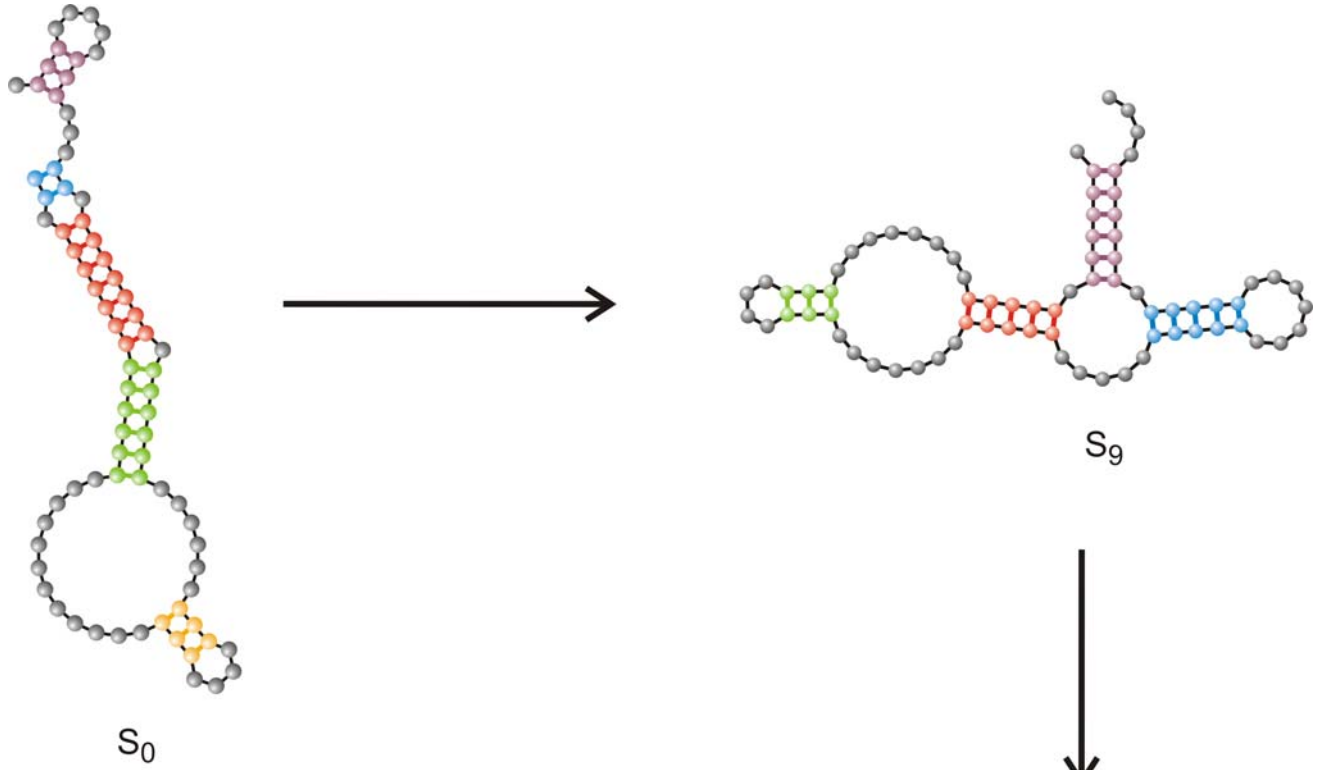

Phenylalanyl-tRNA
as target structure

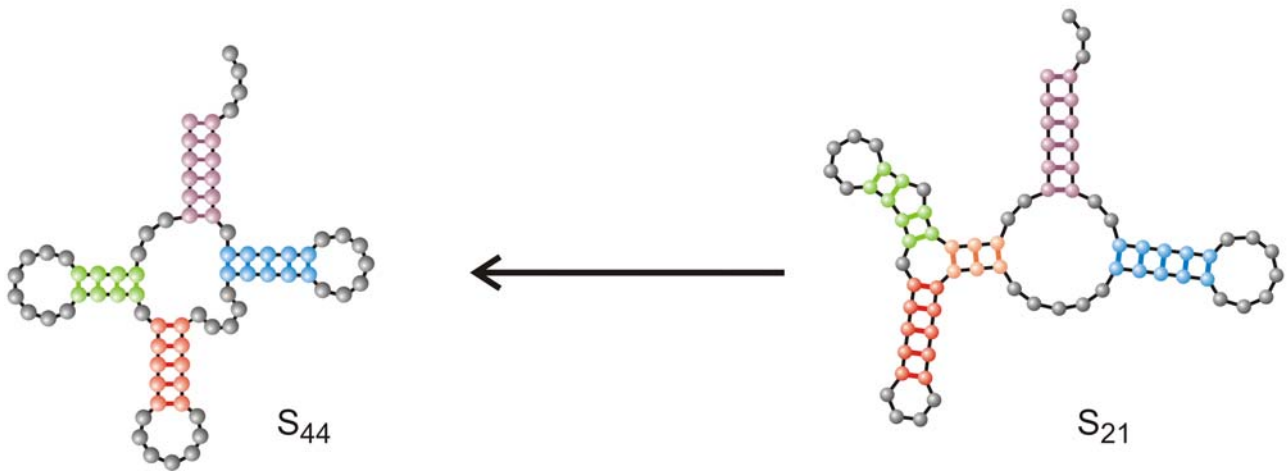

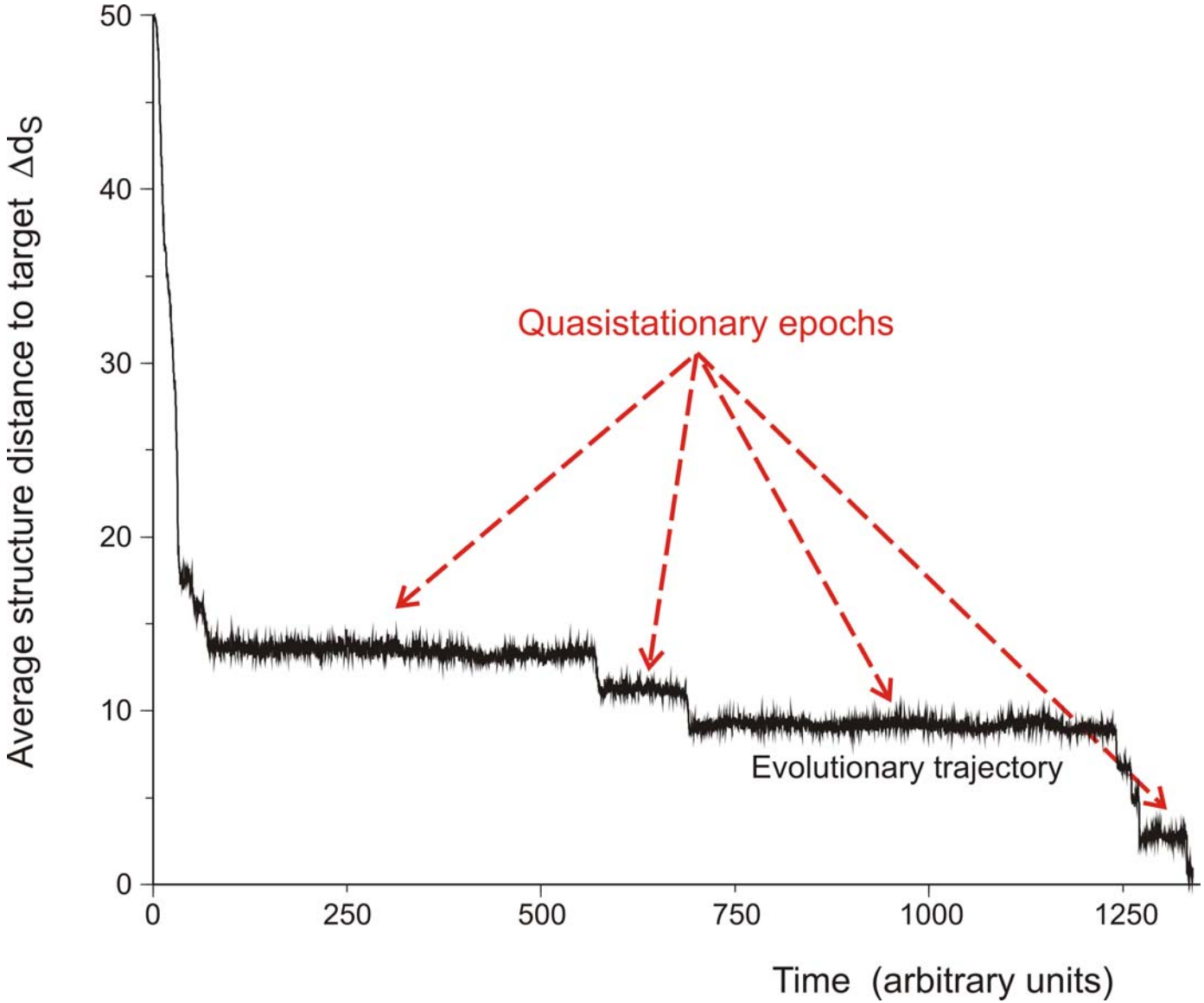

In silico optimization in the flow reactor: Evolutionary Trajectory

28 neutral point mutations during a long quasi-stationary epoch

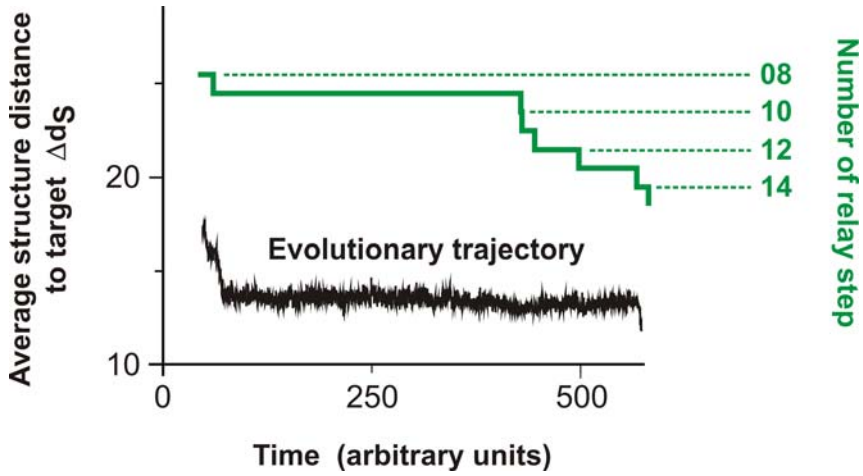


```
entry   GGUAUGGGCGUUGAAUAGUAGGGUUUAAACCAAUCGGCCAACGAUCUCGUGUGCGCAUUUCAUAUCCCGUACAGAA
8       .((((((((((((.........(((....)))).......)))))).....((((.......))))))))))....
exit    GGUAUGGGCGUUGAAUAAUAGGGUUUAAACCAAUCGGCCAACGAUCUCGUGUGCGCAUUUCAUAUCCCAUACAGAA
entry   GGUAUGGGCGUUGAAUAAUAGGGUUUAAACCAAUCGGCCAACGAUCUCGUGUGCGCAUUUCAUAUACCAUACAGAA
9       .((((((.(((((.........(((....)))).......)))))).....((((.......))))).))))))....
exit    UGGAUGGACGUUGAAUAACAAGGUAUCGACCAAACAACCAACGAGUAAGUGUGUACGCCCCACACACCGUCCCAAG
entry   UGGAUGGACGUUGAAUAACAAGGUAUCGACCAAACAACCAACGAGUAAGUGUGUACGCCCCACACAGCGUCCCAAG
10      .(((((..(((((.........(((....)))).......)))))).....((((.......))))).))))))....
exit    UGGAUGGACGUUGAAUAACAAGGUAUCGACCAAACAACCAACGAGUAAGUGUGUACGCCCCACACAGCGUCCCAAG
```

Transition inducing point mutations change the molecular structure

Neutral point mutations leave the molecular structure unchanged

Neutral genotype evolution during phenotypic stasis

Evolutionary trajectory

Spreading of the population on neutral networks

Drift of the population center in sequence space

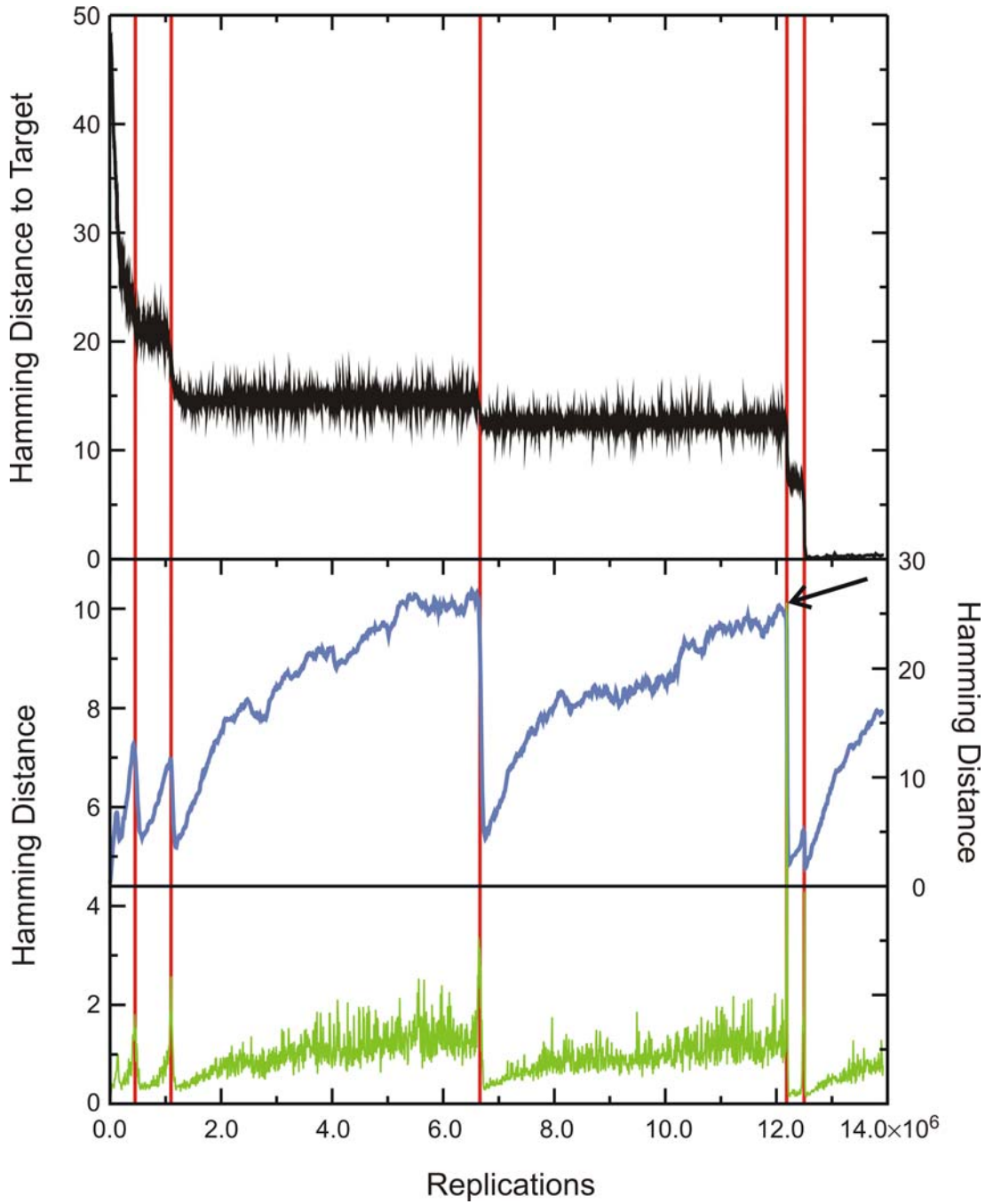

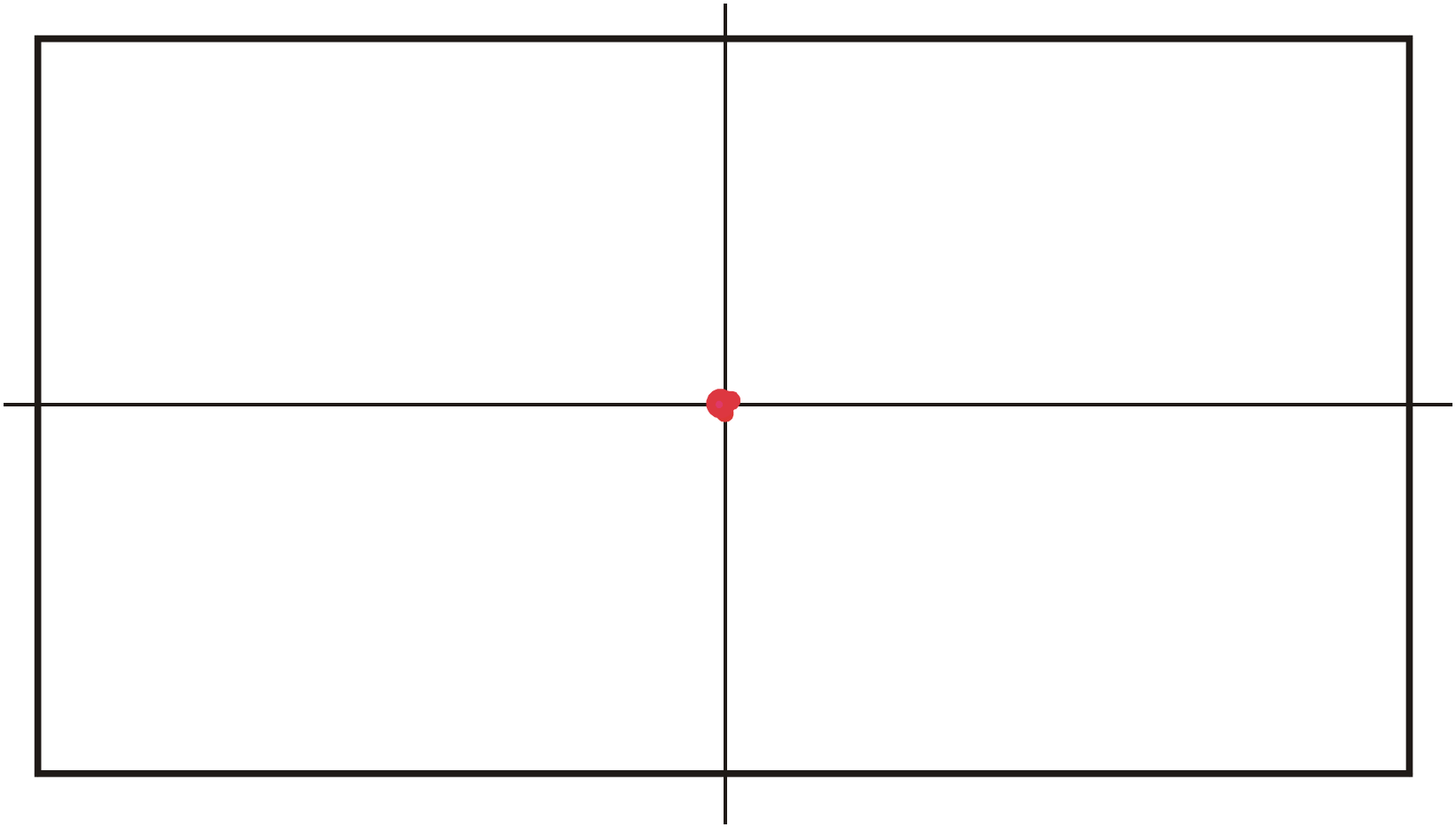

Spreading and evolution of a population on a neutral network: t = 150

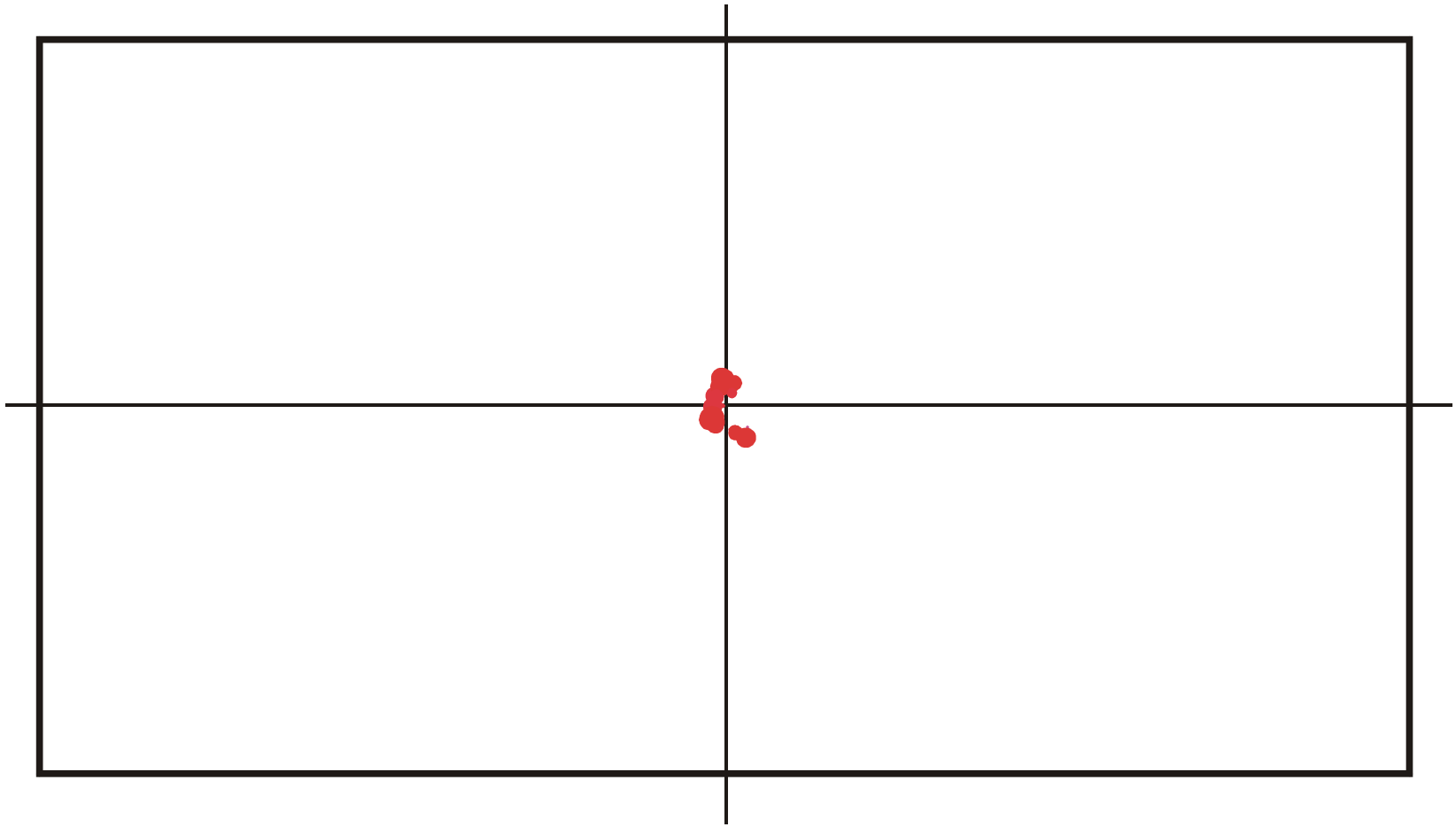

Spreading and evolution of a population on a neutral network : t = 170

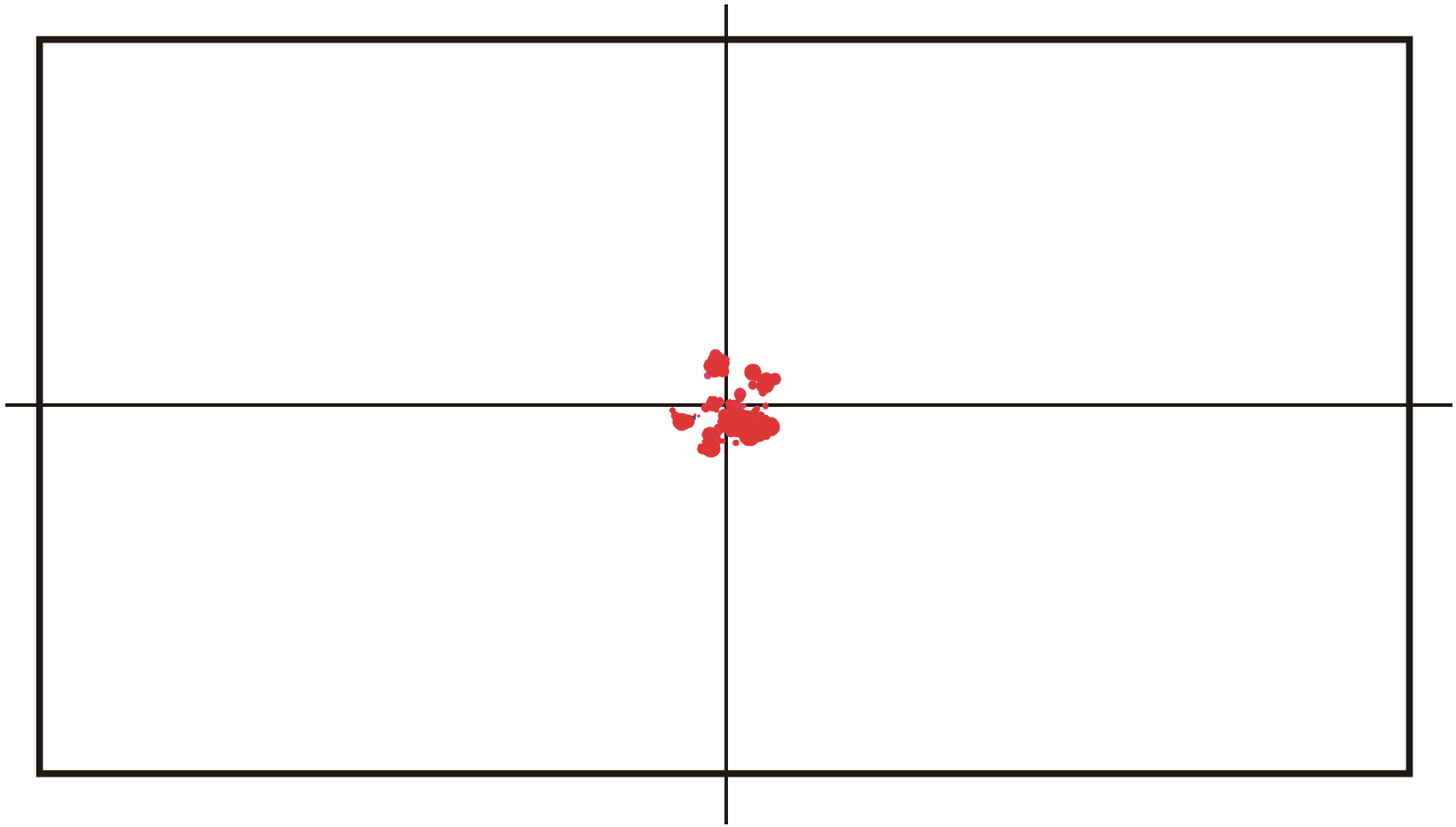

Spreading and evolution of a population on a neutral network : t = 200

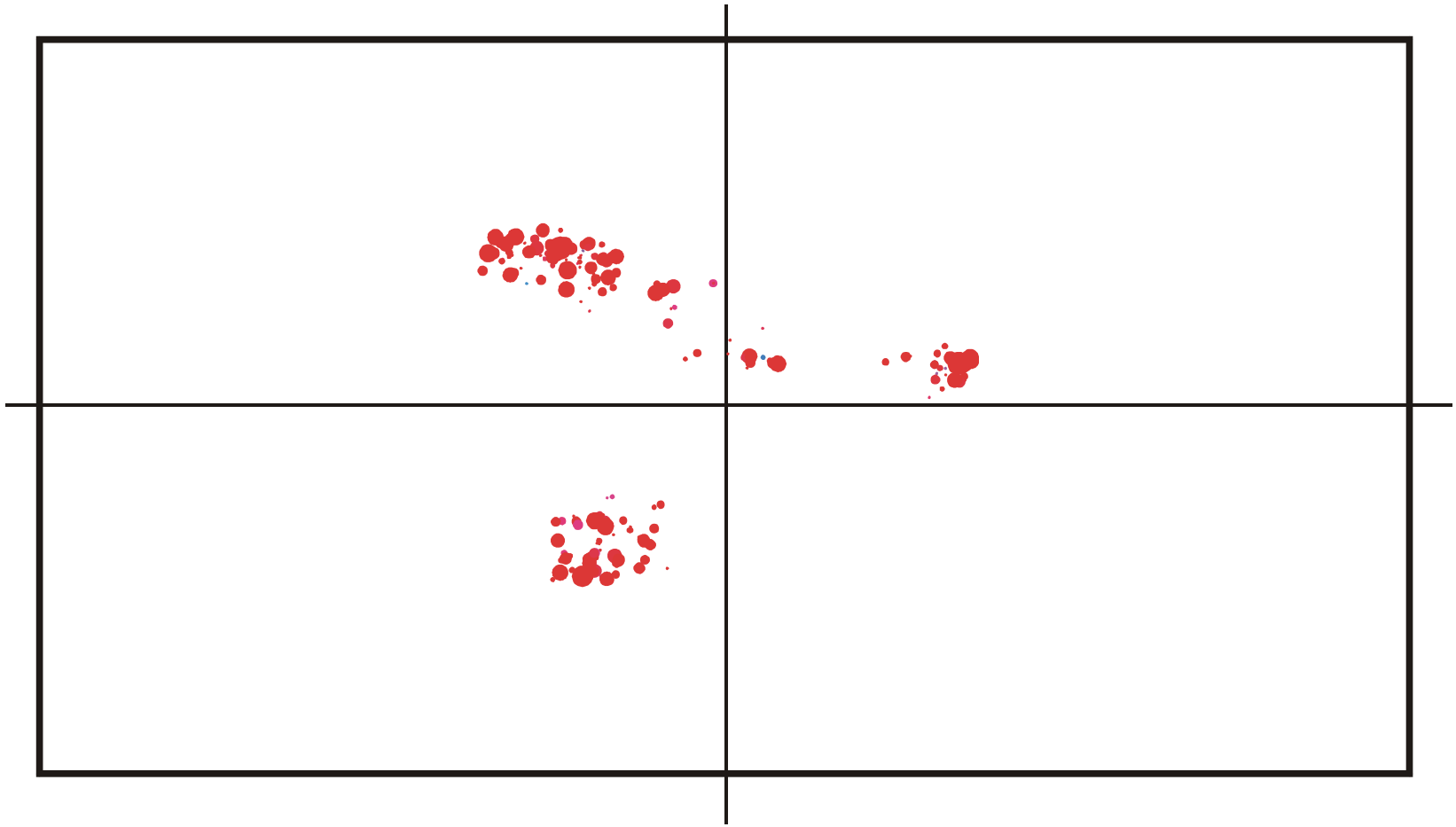

Spreading and evolution of a population on a neutral network : t = 350

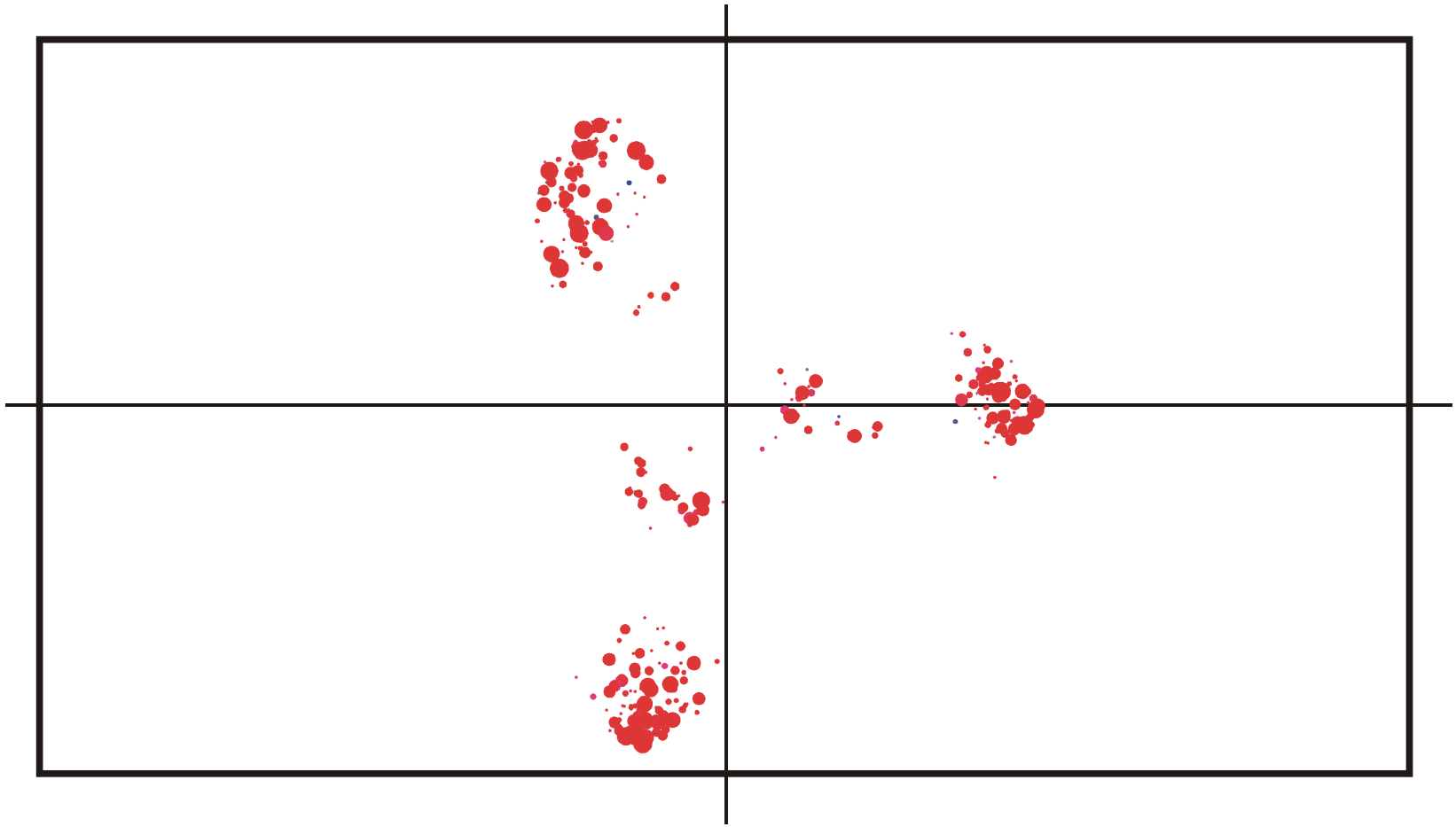

Spreading and evolution of a population on a neutral network : t = 500

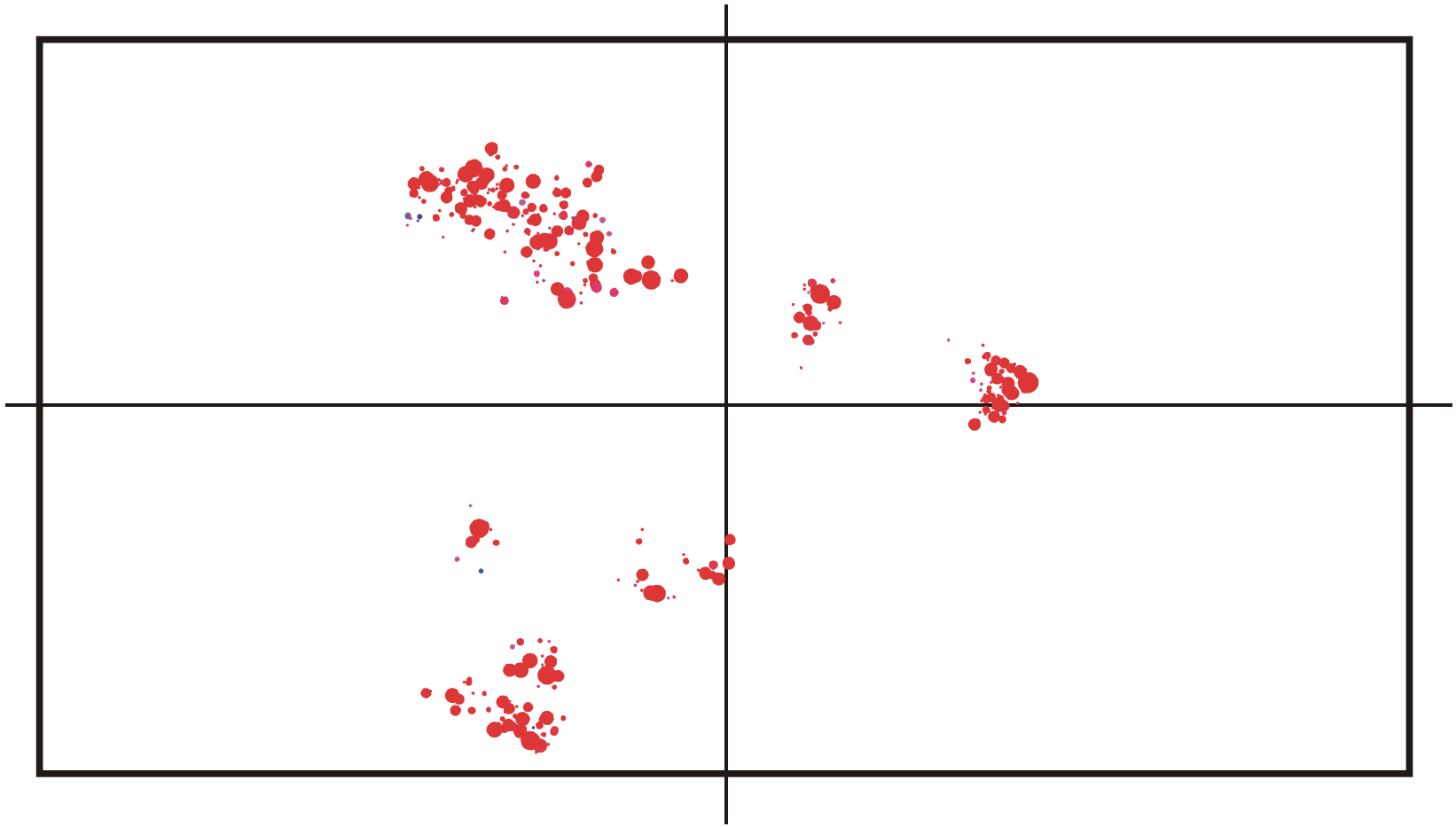

Spreading and evolution of a population on a neutral network : t = 650

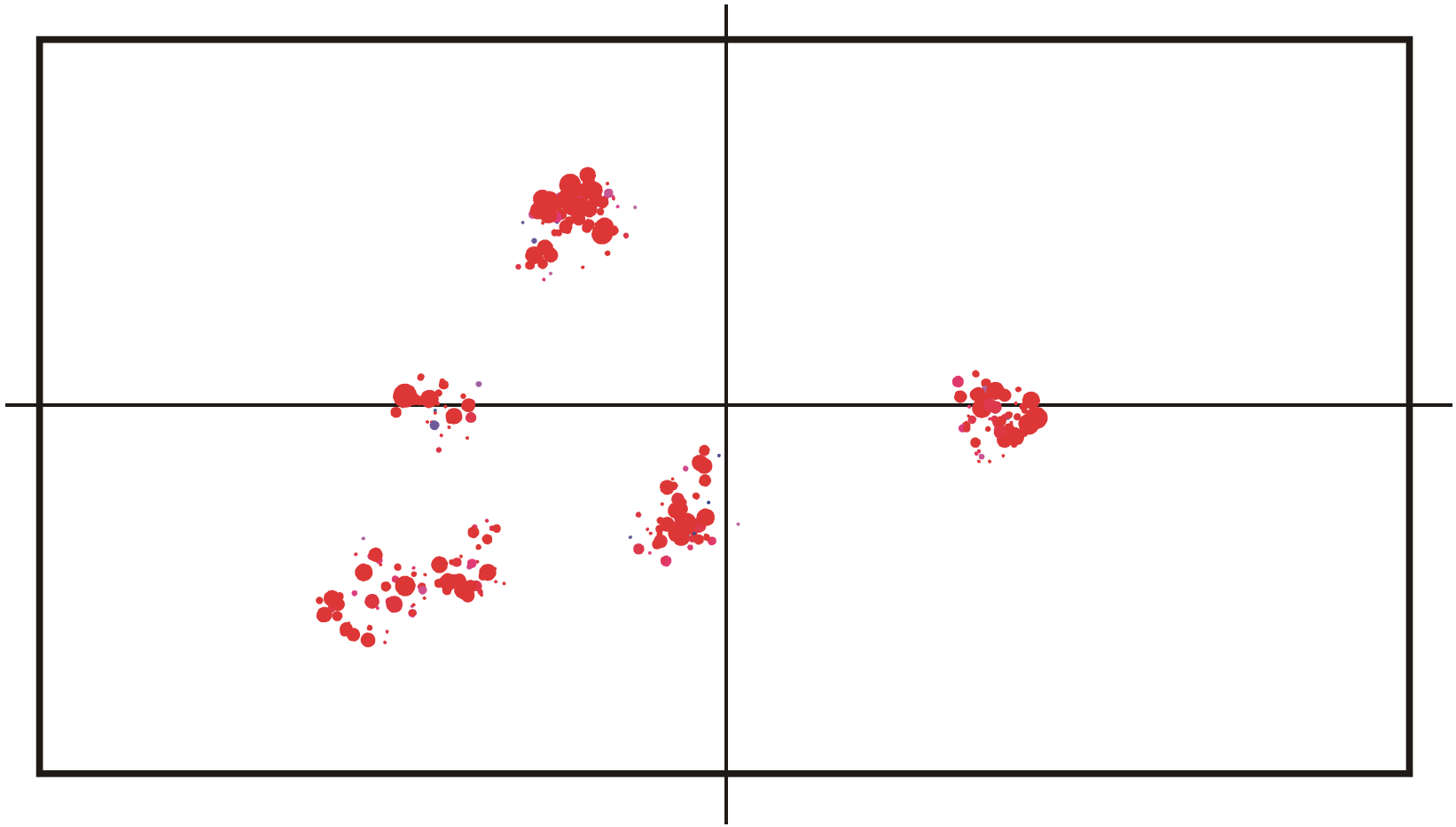

Spreading and evolution of a population on a neutral network : t = 820

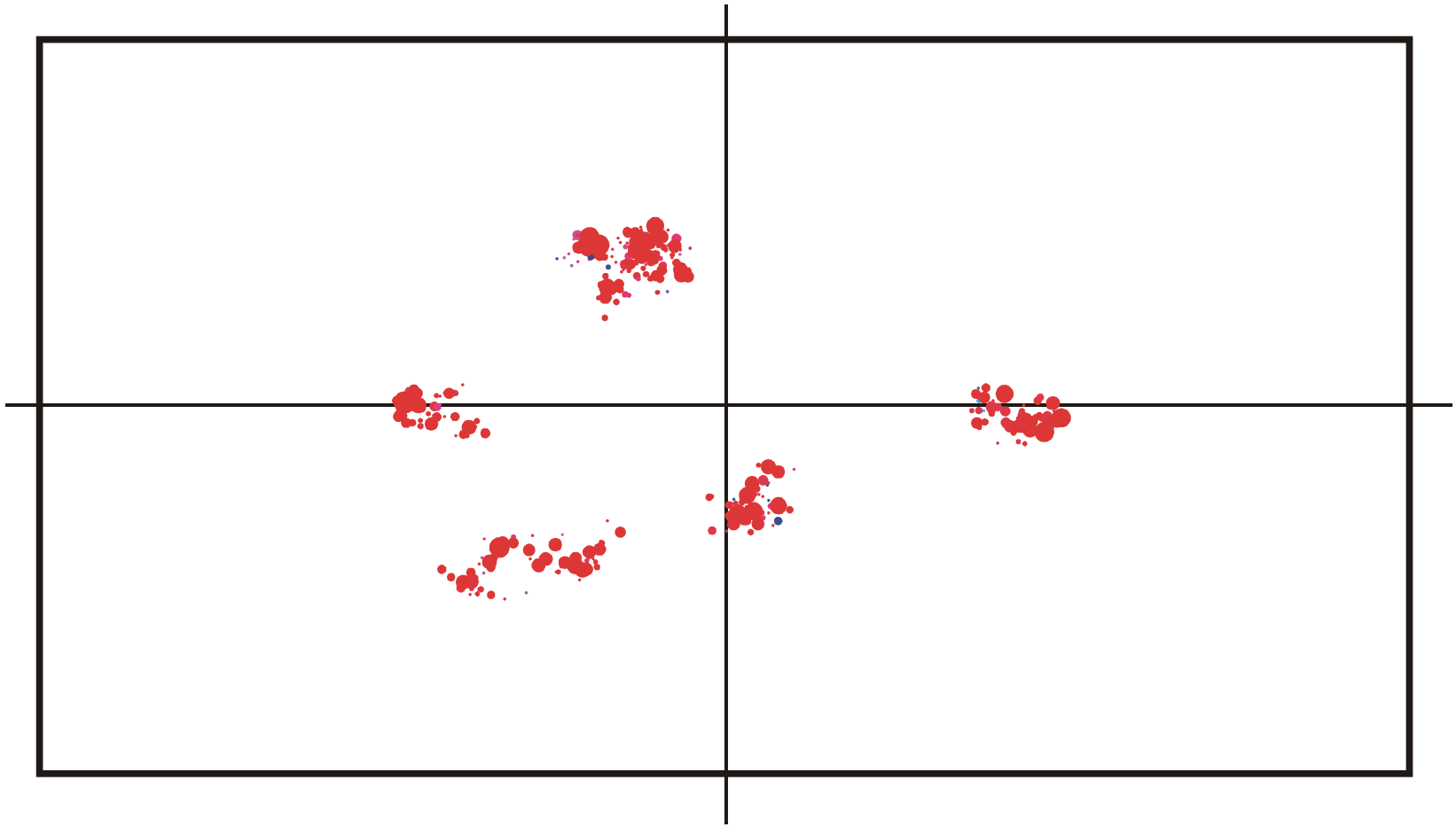

Spreading and evolution of a population on a neutral network : t = 825

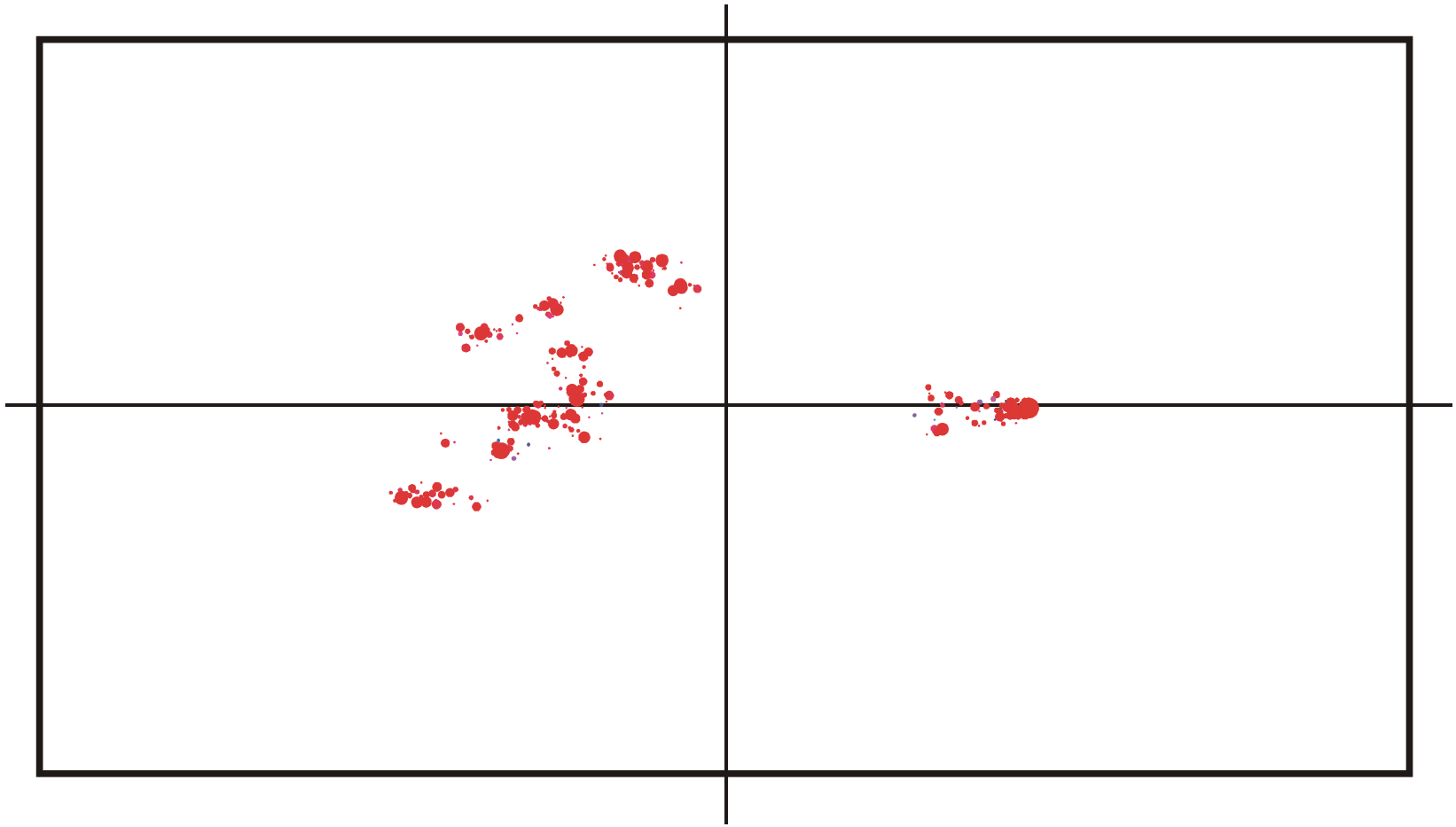

Spreading and evolution of a population on a neutral network : t = 830

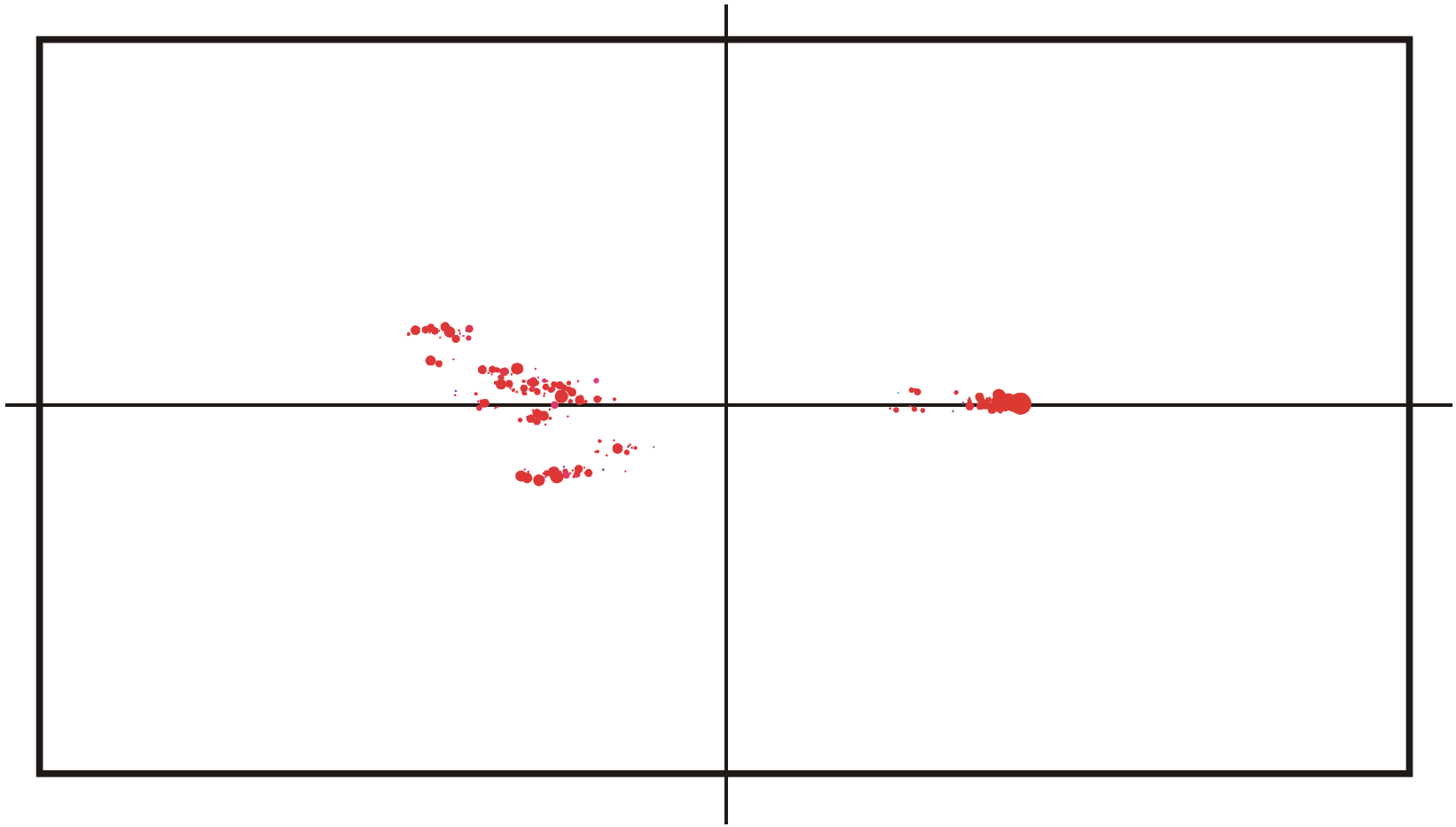

Spreading and evolution of a population on a neutral network : t = 835

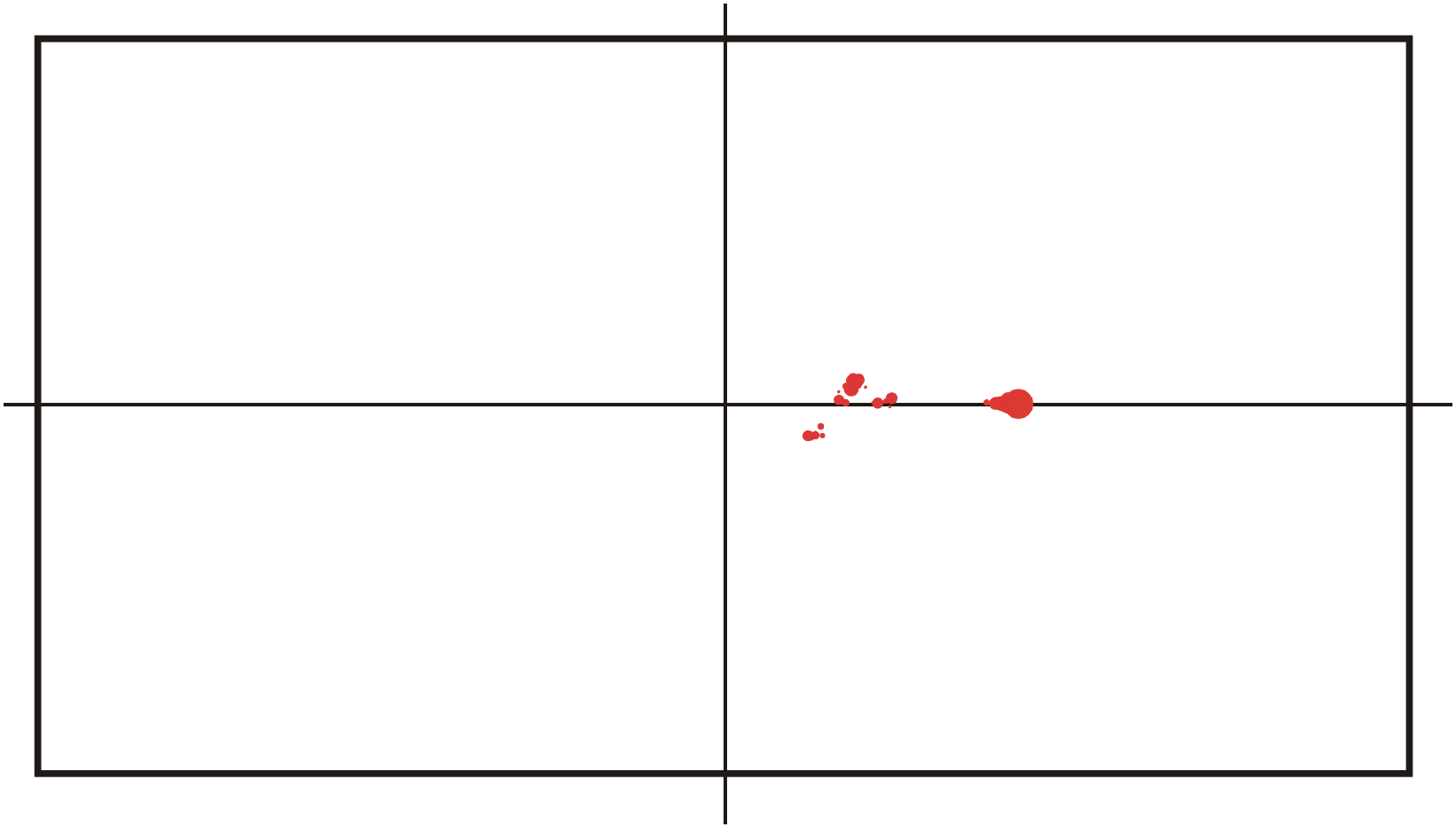

Spreading and evolution of a population on a neutral network : t = 840

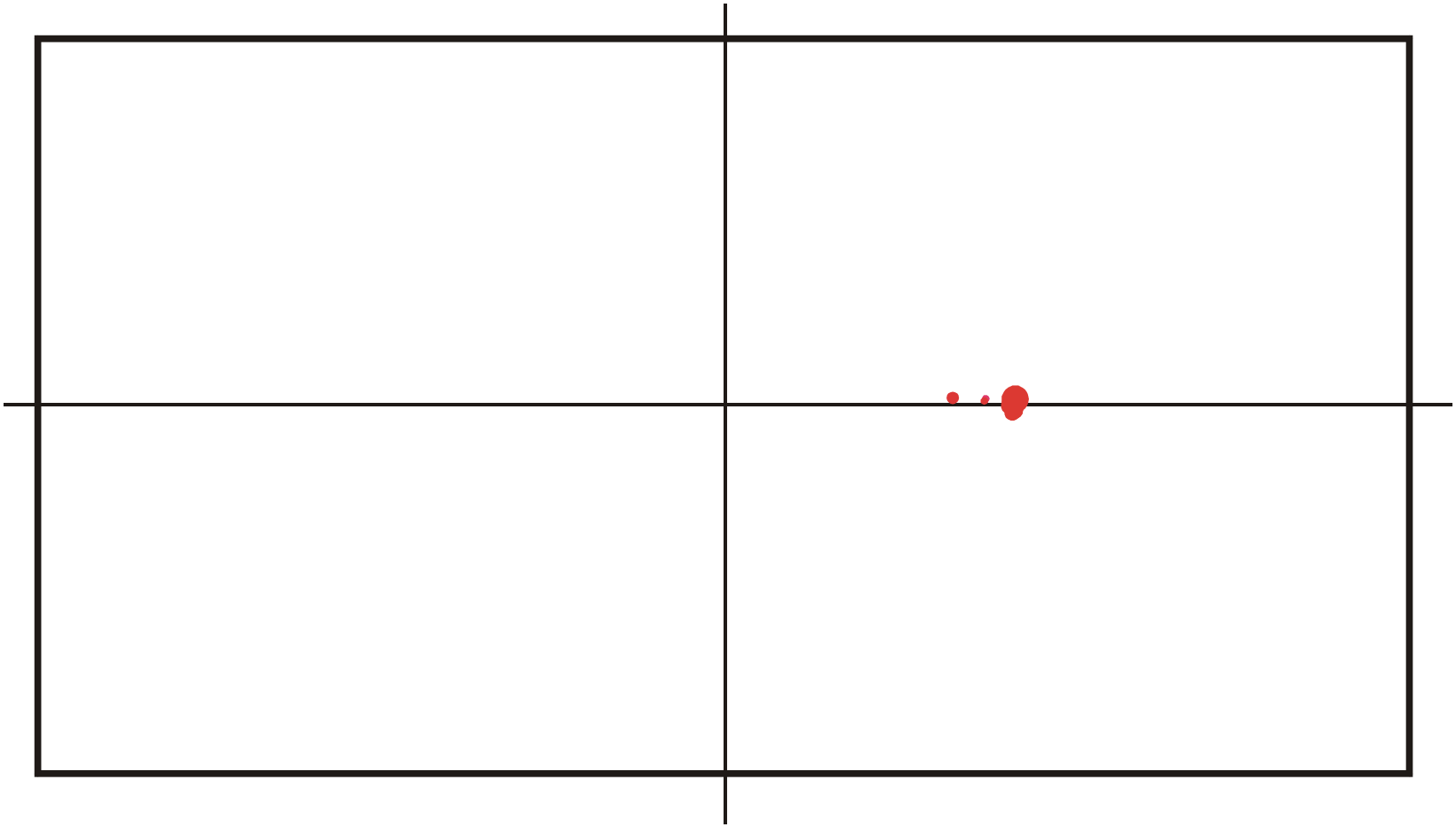

Spreading and evolution of a population on a neutral network : t = 845

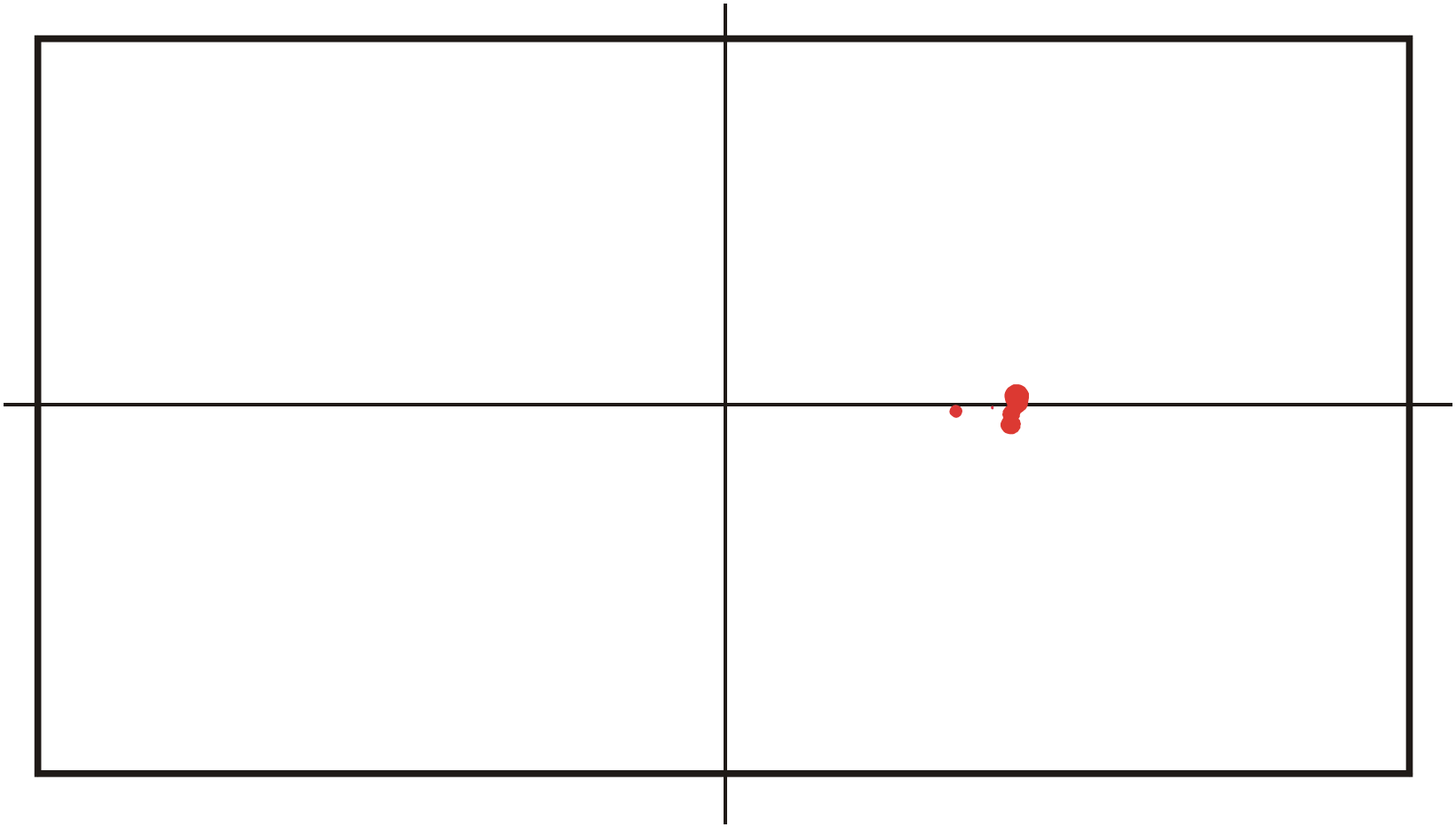

Spreading and evolution of a population on a neutral network : t = 850

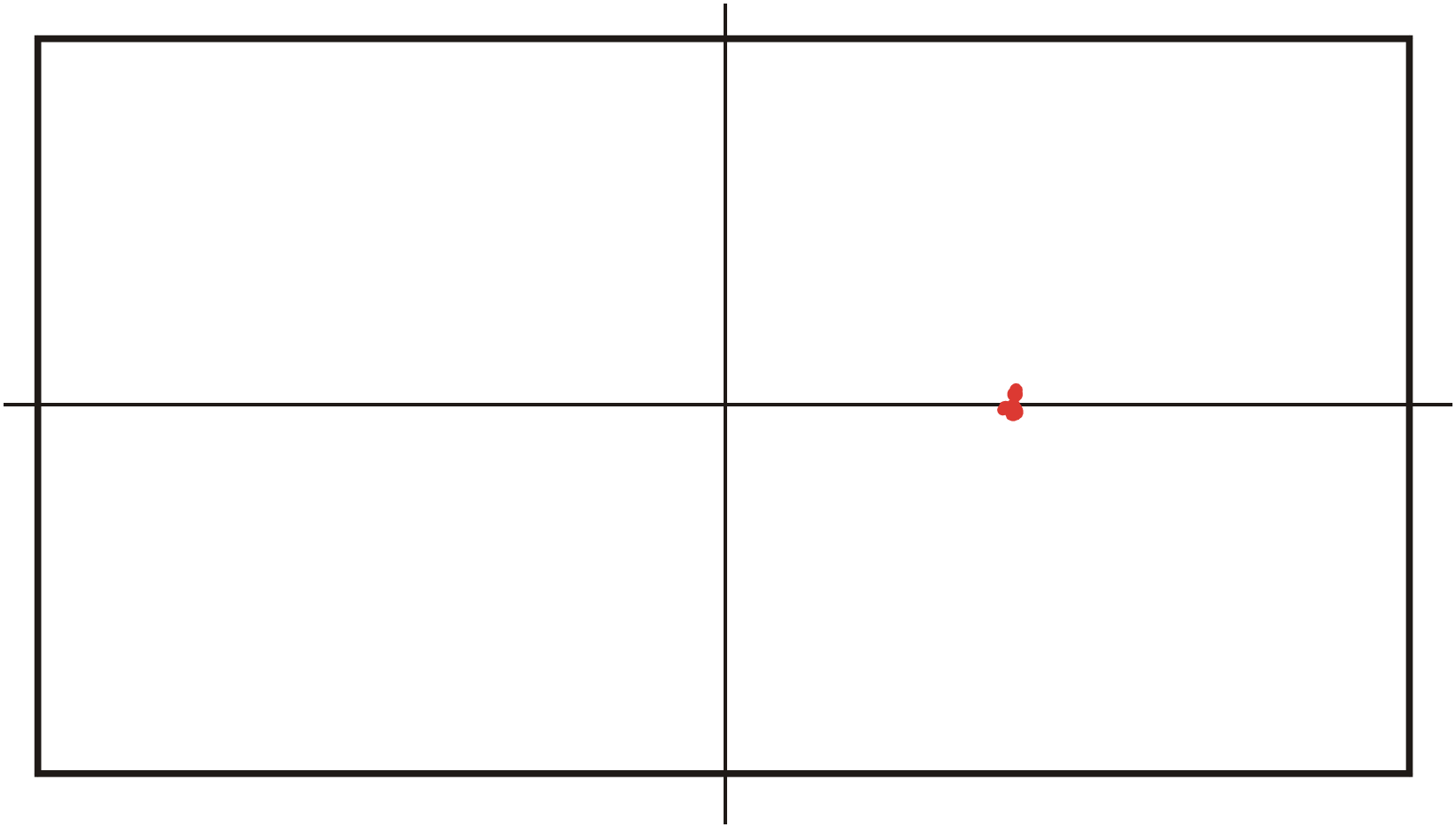

Spreading and evolution of a population on a neutral network : t = 855

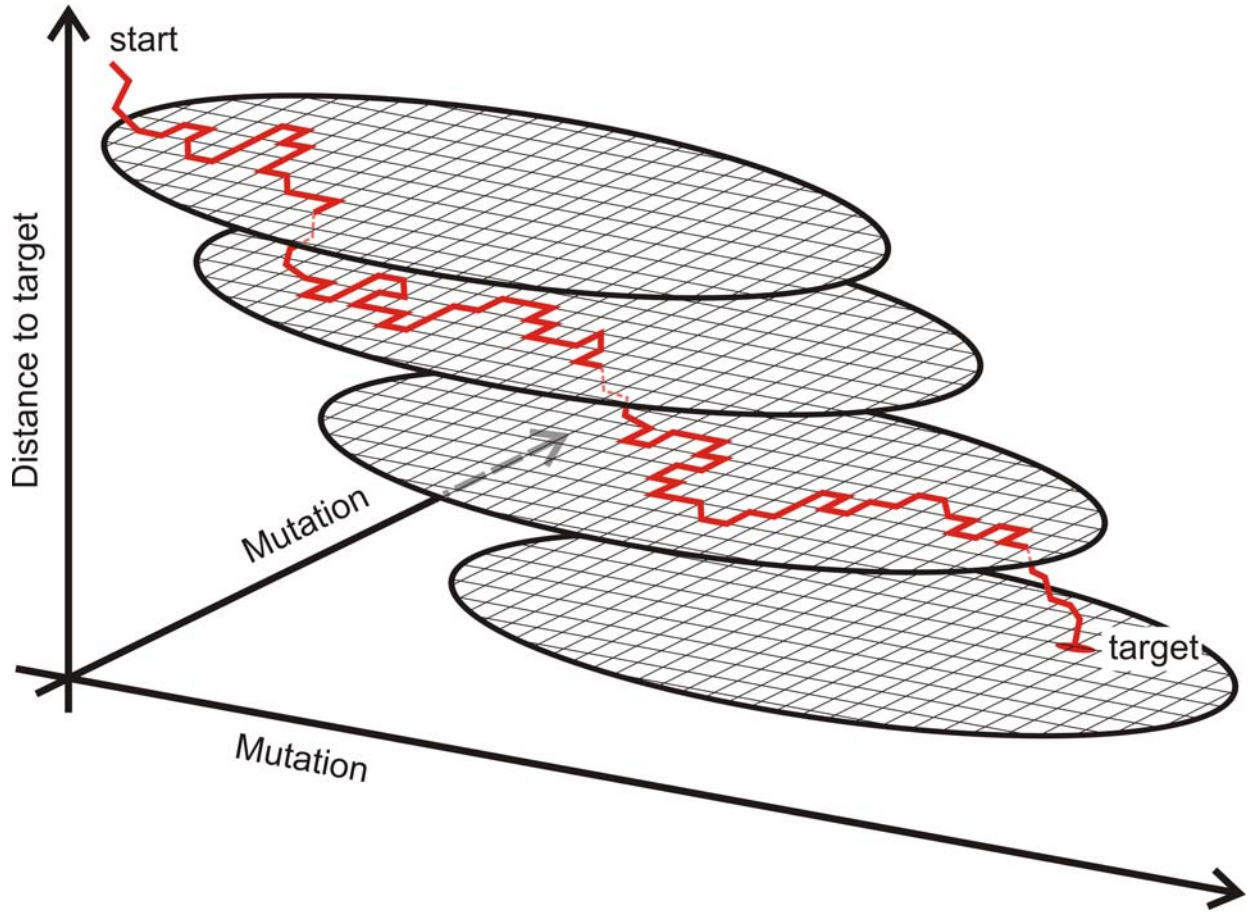

A sketch of optimization on neutral networks

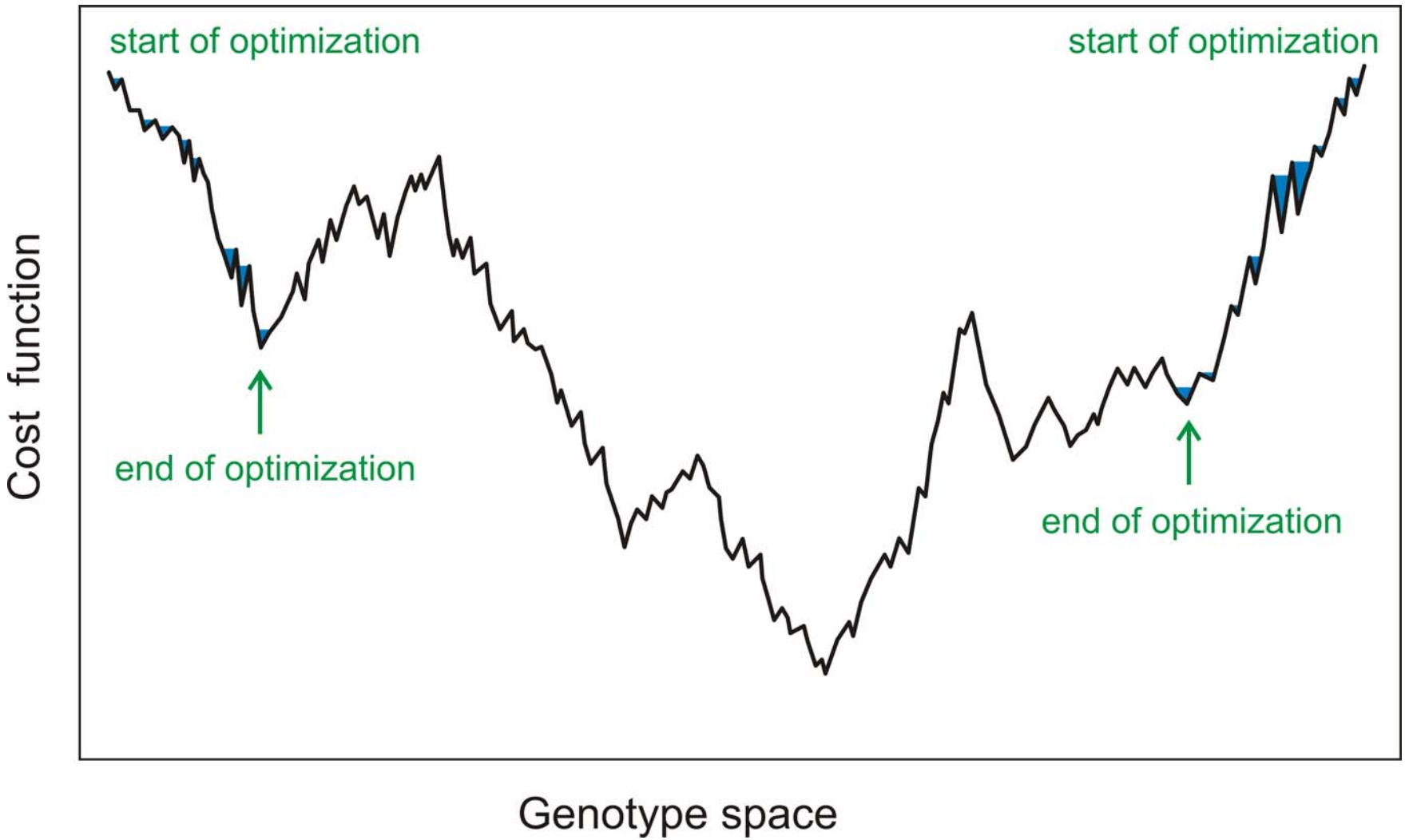
start of optimization
start of optimization
end of optimization
end of optimization
Cost function
Genotype space

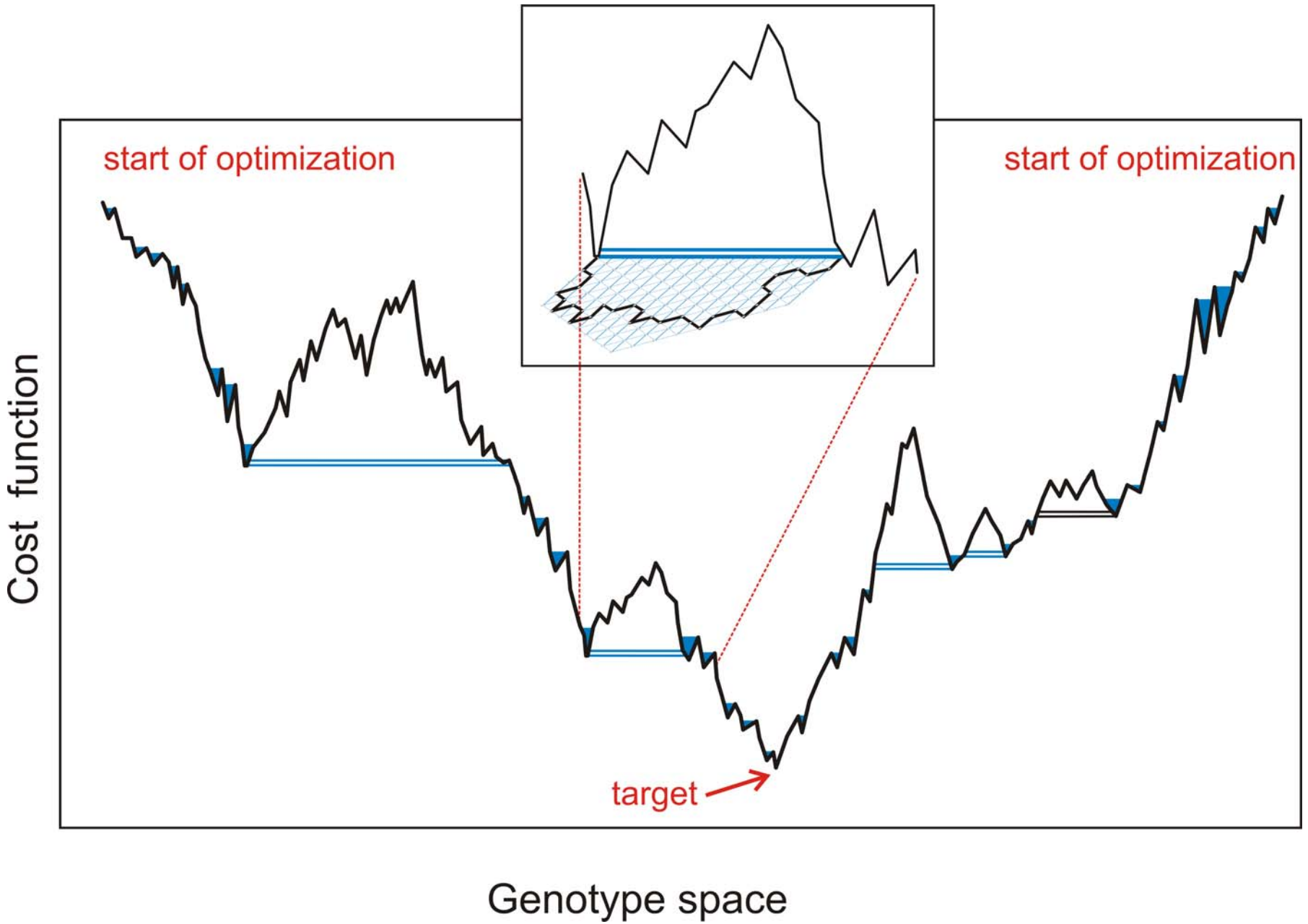
start of optimization
start of optimization
target
Cost function
Genotype space

Acknowledgement of support

Universität Wien

Fonds zur Förderung der wissenschaftlichen Forschung (FWF)
Projects No. 09942, 10578, 11065, 13093
13887, and 14898

Wiener Wissenschafts-, Forschungs- und Technologiefonds (WWTF)
Project No. Mat05

Jubiläumsfonds der Österreichischen Nationalbank
Project No. Nat-7813

European Commission: Contracts No. 98-0189, 12835 (NEST)

Austrian Genome Research Program – GEN-AU

Siemens AG, Austria

Universität Wien and the Santa Fe Institute

Coworkers

Universität Wien

Walter Fontana, Harvard Medical School, MA

Christian Forst, **Christian Reidys**, Los Alamos National Laboratory, NM

Peter Stadler, **Bärbel Stadler**, Universität Leipzig, GE

Jord Nagel, **Kees Pleij**, Universiteit Leiden, NL

Christoph Flamm, **Ivo L.Hofacker**, **Andreas Svrček-Seiler**,
Universität Wien, AT

Kurt Grünberger, **Michael Kospach**, **Ulrike Mückstein**,
Stefan Washietl, Andreas Wernitznig, **Stefanie Widder,**
Michael Wolfinger, Stefan Wuchty, Universität Wien, AT

Stefan Bernhart, **Jan Cupal**, **Lukas Endler, Ulrike Langhammer**,
Rainer Machne, Hakim Tafer, Universität Wien, AT

Ulrike Göbel, **Walter Grüner**, **Stefan Kopp**, **Jaqueline Weber,**
Institut für Molekulare Biotechnologie, Jena, GE

Web-Page for further information:

http://www.tbi.univie.ac.at/~pks